A novel approach to estimate the solubilities of non-steroidal anti-inflammatory drugs (NSAIDs) in supercritical carbon dioxide by PC-SAFT equation of state

(PC-SAFT 状態式に よる超臨界二酸化炭素中の非ステロイド 性抗炎症薬 （NSAIDs）の溶解度推算に向けた新規手法）

Hiroshima University

March 2023

Mahmoud Abdelazim

A novel approach to estimate the solubilities of non-steroidal anti-inflammatory drugs (NSAIDs) in supercritical carbon dioxide by PC-SAFT equation of state

(PC-SAFT 状態式に よる超臨界二酸化炭素中の非ステロイド 性抗炎症薬 （NSAIDs）の溶解度推算に向けた新規手法）

March 2023

Mahmoud Abdelazim

Abstract

Supercritical carbon dioxide holds several advantages over conventional solvents such as being in-toxic, non-flammable, non-polar, and available solvent. It also has mild critical temperature and pressure, low surface tension, and low viscosity and is easy to remove and recycle making it an environmentally friendly material. Owing to these characteristics, supercritical carbon dioxide has found applications in the pharmaceutical industry such as in particle formation, recrystallization, adsorption processes, and the production of sustained delivery devices for controlled release applications.

The knowledge of solubility data is fundamental to understanding any industrial process that employs supercritical carbon dioxide. However, the study of solubility is challenging due to multiple obstacles like the difficulty of conducting the necessary experimental work owing to high cost, the huge number of pharmaceutical materials involved, and their complex structural formula, in addition to their thermal sensitivity that leads to their degradation at high temperatures. Thermodynamic modeling is also challenging due to the limited experimental data present in literature, and the limitations of the popular modeling approaches as they either require experimental solubility data or prior knowledge of the values of some physicochemical properties of the drugs that are hard to measure.

In this study, we suggest a novel thermodynamic method to investigate the solubility of pharmaceutical compounds in supercritical carbon dioxide that combines both experimental and simulation work. This method uses the perturbed chain statistical associating fluid theory (PC-SAFT) which has higher predictive potential than the

commonly used methods that employ cubic equations of state or semi-empirical density equations. The values of the needed three pure component parameters for the investigated drugs are determined using the more readily available and easier-to-measure solubility data in organic solvents. After then, these parameters are used to estimate the solubility of three model non-steroidal anti-inflammatory drugs (ibuprofen, ketoprofen, and salsalate) in supercritical carbon dioxide.

Calculations with PC-SAFT were performed over an extended range of pressures and temperatures for each of the investigated drugs with the binary interaction parameter k_{ij} once set to zero, and once used as an additional adjustable parameter. It was found that PC-SAFT was able to reproduce the experimental values satisfactorily. Additionally, a generalized equation for k_{ij} was derived and then used successfully to describe the isobaric solubility of the studied drugs in supercritical carbon dioxide.

Table of Contents

Chapter 1 : Introduction to the supercritical deposition method

1.1. What is a drug delivery system?

Drug delivery is a technique of delivering medication to a patient so that the drug concentration is specifically increased in some parts of the body than others, and drug delivery systems (DDS) is the device used to achieve such goal. The main aim of using DDS is to reach the targeted site of action with minimal effect on non-target cells, organs, or tissues[1][2].

APIs (active pharmaceutical ingredients) are seldom used clinically in a direct way and are often formulated with other additives to form what is called a dosage form. Examples of traditional dosage forms include pills, ointments, injections, and syrups [3]. APIs are classified according to the Biopharmaceutics classification system into four different classes based on their solubility in water and their intestinal permeability as shown in **Figure 1-1** [4]. It is notable that most of the new drug candidates are of poor bioavailability (i.e., the human body can only absorb a limited amount of them due to their poor solubility in water), which is a challenge that needs to be tackled [5].

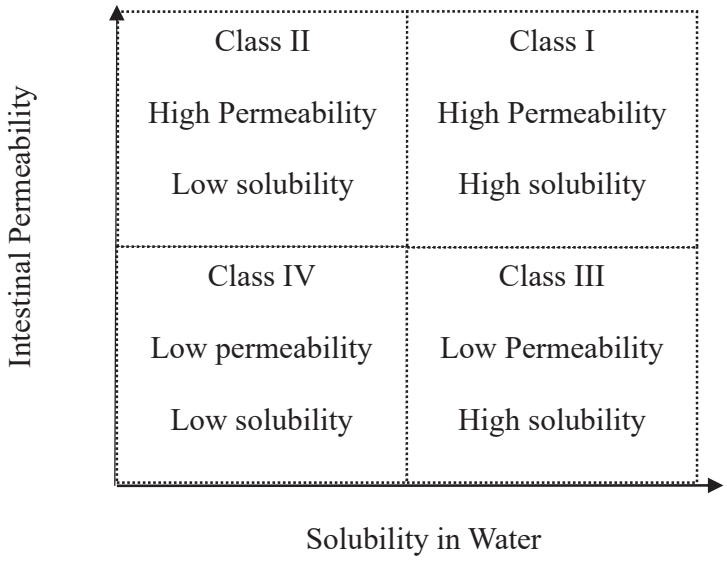

Figure 1-1. Classification of drugs [4]

1.2. What are the kinds of drug delivery systems?

Drug delivery systems (DDS) can be classified into conventional and controlled systems, where conventional DDS include the previously mentioned dosage forms (pills, tablets, injections, and syrups), they have the advantages of being convenient, non-invasive, and of low cost. Their main disadvantage is the fast metabolization after the administration of a single dose, as a result, the drug concentration sharply increases followed by an immediate exponential decrease which could lead to the lack of therapeutic effect [3].

Solutions to this problem include the usage of multiple doses or administering a single dose that is higher than the required dose, both approaches could lead to poor patient compliance or into adverse results such as toxicity and fluctuations in the drug level in the body. Among other disadvantages of controlled DDS are not being target-specific, low

bioavailability, and premature excretion from the body. One potential solution to these challenges is controlled drug delivery [6].

Controlled drug delivery is a process where only the affected area of the human body is targeted with the drug, and where the rate of the release of the drug is controlled according to the patient's condition [7]. Controlled drug delivery holds several advantages over traditional drug delivery such as being target-specific, using a limited quantity of the drug, having a shorter treatment period, improved bioavailability, and better patient compliance [8]. On the other hand, Controlled drug delivery systems are more expensive and may need an invasive procedure to be implanted or removed. Control drug delivery systems have several applications such as polymer implants [9], ocular delivery [10], and tissue engineering[11].

Controlled drug systems can be classified according to the mechanism by which the drug is released from the dosage form into dissolution-controlled, diffusion-controlled, water penetration-controlled, chemically controlled, and nano-particle-based systems [3]. Supports used in controlled drug delivery include polymers, lipids, ceramics, inorganic and porous materials [12].

The use of nanocarriers in drug delivery systems has gained more popularity in recent years. Nanocarriers can reach remote sites and tissues including crossing the blood-brain barrier, can enhance the bioavailability of drugs, and have improved tumor penetration for anti-cancer drugs. Nanocarriers include liposomes, metal nanoparticles, carbon nanotubes, and mesoporous silica nanoparticles [13]. Mesoporous materials possess a high pore volume with a narrow diameter distribution, a high surface area, also their pore size can be tailored according to the used drug. As a result, mesoporous materials can be utilized with a wide

range of drugs, and the release of the drug from them can be predicted and controlled making them a good fit for controlled drug delivery applications[14].

1.3. How are controlled drug delivery systems manufactured?

Different methods are used to manufacture controlled drug delivery systems, they mainly fall into two categories: conventional methods and supercritical methods.

1.3.1. Conventional methods

Conventional methods include simple mixing, extrusion, spray drying, solvent-based techniques, co-spray drying, and microwave radiation [12]. Physical mixing involves blending both the drug and the carrier to produce a dispersion [15]. The solvent-based techniques are the most used conventional method, firstly the drug is dissolved in the chosen organic solvent, next the solvent is contacted with the carrier for an extended period and finally, the solvent is evaporated [16]. Another method is the melt technique which is a solvent-free process that melts both the drug and carrier to obtain a physical mixture. These methods involve some disadvantages such as the usage of large amounts of organic solvents whose processing entails an economic and environmental cost, require filtration or drying steps, are energy and time-consuming, and possibly might contaminate the product with residual traces of the used solvent. In addition, some of them use high temperatures that may cause thermally sensitive drugs to disintegrate [17].

As a result, other conventional approaches have been proposed such as co-spray drying where the carrier is dispersed in a solution of the drug in a volatile solvent followed by the spray drying of the dispersion. While the product of this process has improved oral

bioavailability and is more stable, but it has the typical drawbacks attributed to the usage of an organic solvent [18]. Another solution to the drawbacks of the conventional methods is the supercritical deposition method which will be discussed in the following section.

1.3.2. Supercritical deposition method

A supercritical fluid can be defined as any fluid at conditions above its critical temperature and pressure, it is considered an intermediate phase between liquid and vapor, they exhibit outstanding properties such as gas-like viscosity and diffusivity and liquid-like density and solvating properties. Supercritical carbon dioxide is one of the exploited supercritical fluids owing to its abundance, non-flammability, and mild critical coordinates (its critical temperature is 31.25^0C and its critical pressure is 7.38 MPa) [23].

$ScCO_2$ is chemically inert, non-toxic, has low critical temperature which facilities the processing of thermally labile drugs and eliminates the need for high processing temperatures, it also has low viscosity and surface tension which eases the penetration of the drug into the used carrier and thus the loading of higher concentrations of the drug into the carrier if compared with conventional methods [19]–[21]. The properties of $scCO_2$ can be manipulated easily by changing its temperature and pressure leading to easy removal from the process medium and subsequent recycling [23]. This last feature limits the environmental impact of the process and ensures a solvent-free product [24].

The supercritical deposition method uses supercritical fluids as its solvent of choice and benefits from their attractive features of them to produce drugs with superior purity while inflicting minimal impact on the environment. The supercritical deposition process reduces the number of required stages even though there are extra costs associated with the process

in order to provide the necessary pressure. It is worth mentioning that supercritical carbon dioxide ($scCO_2$) is the most used solvent in this process[24].

Supercritical deposition consists of three main steps; dissolution where the target drug is dissolved in the supercritical fluid. Next, the dissolved drug is contacted with the support to adsorb the drug into the support. Lastly, a gradual release of pressure is allowed to separate the loaded drug from the supercritical fluid and attain the final product [2],[24]. The different stages of the supercritical deposition process are illustrated in **Figure 1-2**.

In this work, we are going to investigate the first stage of the supercritical deposition process through an approach that combines both experimental work and thermodynamic modelling, and that makes use of the available data in the literature to tackle some of the challenges related to the development of controlled drug delivery systems.

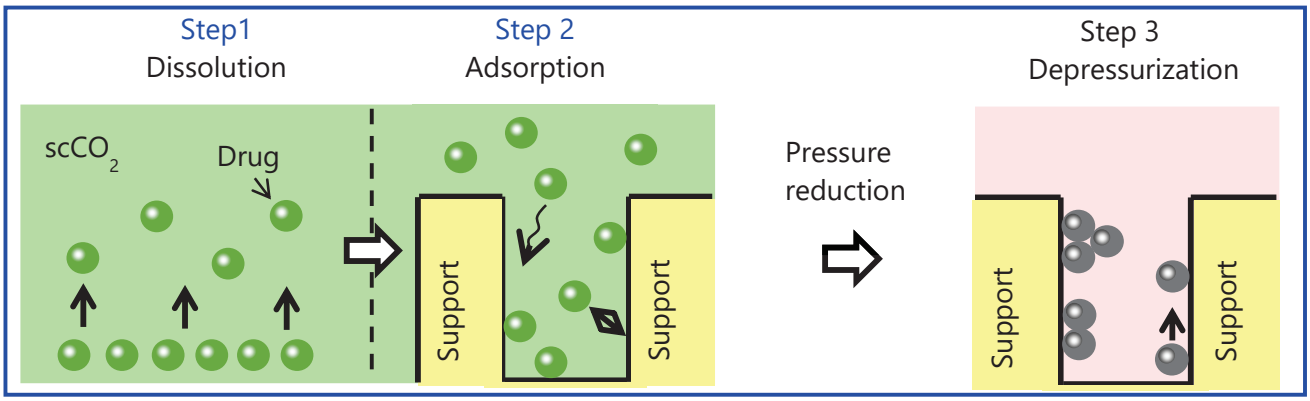

Figure 1-2. The stages of the supercritical deposition process

1.4. An overview of the proposed approach in this work

To acquire a good understanding of the process of manufacturing-controlled drug delivery systems using the supercritical deposition method, experimental work is crucial. The experimental work provides values that are necessary to understand the system under different operating conditions and with different drugs used. Measurements for the pure component properties of the drugs are also fundamental to developing thermodynamic models that can be used for the design and operation of engineering processes that include supercritical fluids.

Drugs are thermally sensitive materials that may decompose at high temperatures and need special treatment when conducting experimental work. The number of drugs that need to be investigated is vast and is increasing every year due to the addition of new drugs. Furthermore, the typically high cost of conducting experimental work is further exacerbated by the expensive price of some of the candidate drugs. Moreover, the systems investigated are non-ideal systems that involve high pressures and low drug concentrations which raise the need for sensitive equipment and skilled personnel to conduct the experiments. It can be concluded that the experimental work needed to measure the solubility of solid drugs in $scCO_2$ is challenging.

One potential solution that would reduce the required experimental load is the development of thermodynamic models that can produce the necessary data for the development, design, and operation stages of the supercritical deposition process. Several methods are used to investigate the solubility of solid APIs in $scCO_2$, with the methods employing equations of state (EoS), and semi-empirical density equations being the most

popular [25], [26]. Both approaches have different characteristics and their own set of advantages and disadvantages that will be discussed in detail in **Chapter 2.** Numerous scholars have applied the EoS approach to study the solubility of APIs in $scCO_2$ using equations such as Peng Robinson (PR) EoS, Soave-Redlich-Kwong (SRK) EoS, and modified Pazuki EoS along several mixing rules [27]–[31]. These equations are based on the corresponding state principle and require pure component properties of the drug such as the acentric factor or critical properties that are difficult to measure for pharmaceutical compounds and thus, are estimated using methods such as group contribution methods, which raises the possibility of the introduction of more errors to the calculations. On the other hand, the semi-empirical equations require experimental solubility data to be fit into to determine the value of their parameters. As a result, they have limited predictive power and are only capable of conducting correlation based on experimental results. In addition, the bulk of the produced publications focus more on the measurement of solubility and then its correlation with less focus being directed toward solubility estimation. Therefore, a new thermodynamic model is needed to develop more understanding of the solubility of solid drugs in $scCO_2$.

Perturbed-chain statistical associating fluid theory (PC-SAFT) [32], [33] is an equation of state that combines perturbation theory and molecular thermodynamics and is a potential candidate for the estimation of the solubility of APIs in $scCO_2$. This can be attributed to the advantages it possesses due to its statistical mechanics background such as the possibility of using molecular simulations to invalidate it, and the possibility of improving the obtained results by modifying the terms of the EoS according to the investigated system. Finally, the terms of PC-SAFT have physical meanings that make the derivation of new parameters for

the studied systems based on the original one an easier task[34].

In this study, we chose to conduct the investigation on three of the most used non-steroidal anti-inflammatory drugs (NSAIDs): ibuprofen, ketoprofen, and salsalate. These drugs are available and are commonly used by researchers around the world facilitating the replication and validation of the produced results. The perturbed-chain statistical associating fluid theory is the basis of the thermodynamic model, it was selected due to its solid statistical background, predictive power, and its success in dealing with other complex systems such as polymer systems [35], biofuels [36], and ionic liquid [37].

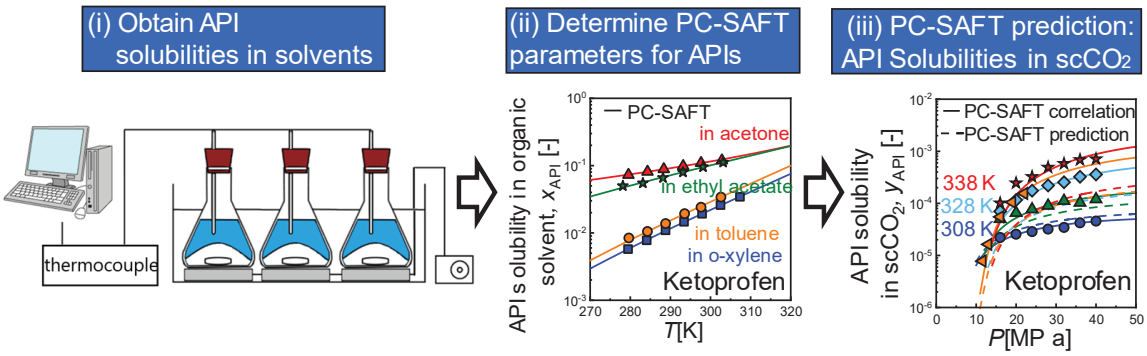

Figure 1-3. Schematic of the proposed approach

To perform calculations by PC-SAFT, the values of the pure parameters (segment diameter σ_i, segment number m_i, and dispersion energy μ_i) for each component i in the system are needed, when the effect of association by hydrogen bonds is absent in the studied system. Usually, those parameters are determined via the fitting of vapor pressure and liquid density data for the pure components [33], [38], but this is difficult for solid APIs as many of

them decompose at elevated temperatures.

For the first stage (dissolution), we propose to extend the method proposed by Paus et al. [39] to determine the PC-SAFT pure component parameters for several solid APIs in aqueous solutions into supercritical fluids, this extension has not been evaluated to date, and will be assessed in this work. In this approach, measurements of the solubility of the APIs in organic solvents are carried out; these measurements are easier to conduct than those in supercritical fluids and more results are published in the literature paving the way for a predictive approach that uses the available data. Based on those measurements, the required PC-SAFT pure component parameters for the drugs are determined. The next step is using these parameters along PC-SAFT to estimate and correlate the solubility values of the studied APIs in supercritical carbon dioxide. We used experimental data from the literature for ibuprofen and ketoprofen and experimental data conducted in our lab for ketoprofen and salsalate. A schematic of the proposed research can be found in **Figure 1-3.**

The aims of this research are as follows:

1. Provide experimental results than can contribute to the understanding of the supercritical deposition process of NSAIDs in meso-porous silica supports.
2. Develop a novel thermodynamic model that can be used to model the stage of dissolution of the supercritical deposition method

1.5. The outline of this study

In Chapter 2, a Literature review of the experimental and modeling work for the supercritical deposition will be presented. The different experimental setups will be presented, and the different equations used to conduct the thermodynamic models with the strengths and drawbacks of each method highlighted along the past research effort in literature.

In Chapter 3, the used experimental and thermodynamic approach will be discussed in detail. This study investigated the solubility of the selected NSAIDs in organic solvents at the range of 278-333K and studied their solubility in supercritical carbon dioxide at 8-40 MPa and 308-338K

In Chapter 4, the results of both the experimental work and thermodynamic modeling for the dissolution stage will be presented and discussed. The modeling involved both correlation and estimation efforts whose results will be discussed, and the success of the model in describing the studied system will be evaluated.

In Chapter 5, a summary of the study and recommendations for future research will be presented

Chapter 2 : Literature review of the common experimental setups and thermodynamic models

In this chapter, the present knowledge in the literature related to the first stage of the supercritical deposition process, dissolution, will be discussed. Firstly, the importance of the solubility measurements will be highlighted, and then a review of the experimental setups used to measure solubility will be discussed focusing on the advantages and disadvantages of each. Next, the different thermodynamic approaches will be presented, and their strengths, limitations, and usage will be investigated. Finally, the different thermodynamic approaches will be evaluated.

2.1. The importance of the solubility data

The accurate values of the solubility of APIs in different solvents including supercritical carbon dioxide ($scCO_2$) are essential in the research and development, optimization, design, and operations efforts for not only the manufacture of drug delivery systems but for any process that uses those solvents. Examples of the processes involving ($scCO_2$) include separation and extraction [40], crystallization[41], adsorption[42], particle formation[43] , polymer foaming [44] , and food processing[45] .

Experimental work and thermodynamic modeling are two powerful tools used by scholars to enhance their understanding of the solubility process of APIs in $scCO_2$. The development of reliable thermodynamic models cannot be carried out without accurate experimental data to assess the produced models. These models are invaluable tools to reduce

the number of needed experiments and therefore their cost, to design and operate industrial processes that use ($scCO_2$).

2.2. Experimental setups for solubility measurements in $scCO_2$

The experimental system usually includes three steps: firstly, the introduction of $scCO_2$ into the equilibrium cell, secondly the equilibrium between the solid solute and the $scCO_2$ is attained, and finally, the analysis of the obtained samples is carried out to get the experimental results [38]. The methods to carry out such experiments can be classified into two classes according to the way by which the composition is determined: Analytical methods, where the determination of the equilibrium phase compositions is carried out by analyses after sampling, and synthetic methods where this is done indirectly without sampling. The analytical methods are more common, and they can be mainly divided into static and dynamic methods with each method having its own characteristics advantages, and drawbacks [46].

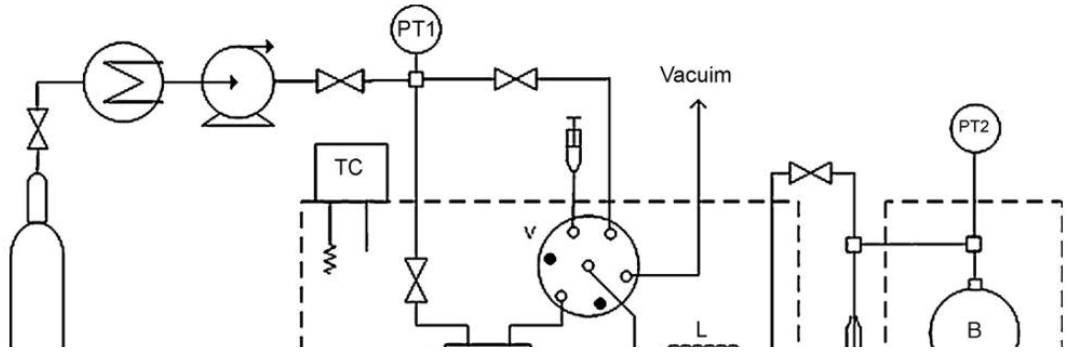

Figure 2-1. Schematic of the static method for solubility measurements in $scCO_2$.
PT1: High pressure transducer, PT2: low pressure transducer, TC: Temperature controller, E:Equilbrium cell, V: six-port sampling value, L: Sampling loop, T: glass trap, B: Expansion balloon [69].

The static method uses closed equilibrium cells of constant or variable volume, recirculation of the solvent may be included in some cases, agitation by a magnetic stirrer to accelerate reaching equilibrium, movable piston or simply keeping the solution in concern in the cell for a fixed duration, a schematic of the static method is shown in **Figure 2-1**.

It is worth mentioning that the static method employs a fixed amount of both solute and solvent. Static method equipment can be equipped with a heating system and a pressure gauge to control both the temperature and pressure of the system and to facilitate the achievement of equilibrium is simple and easy to use, but it has several drawbacks such as the need for separate analysis and being time-consuming [47]

The static method was used extensively to measure the solubility for a variety of APIs in $scCO_2$ at a wide spectrum of pressure and temperature as shown in **Table 2-1**. In addition, the static method was also employed to measure the solubility of solids other than drugs such as the measurement of the solubility of nitrophenol derivatives by Shamsipur et al.[48] and the solubility of pesticides xanthone and xanthene by Huang et al. [49]. That shows the wide usage of the static method to measure the solubility of different drugs at an extended range of temperatures and pressure.

Table 2-1. Examples of measuring the solubility of drugs in $scCO_2$ by the static method

API	Temperature [K]	Pressure [MPa]	Solubility $\times 10^5$	Authors
Deoxycorticosterone acetate	308-348	12.2-35.5	0.01-1.34	Asiabi et al. [50]
Clobetasol propionate	308-348	12.2-35.5	0.01-1.34	Asiabi et al. [50]
Nifedipine	333-373	10-30	0.5-7.1	Knez et al. [51]
Nitrendipine	333-373	10-30	0.6-10.6	Knez et al. [51]
Imatinib mesylate	308-348	10-27	0.05-0.4	Sodefian et al. [52]
Cefixime trihydrate	308-328	18-33.5	0.01-1.6	Khamda et al. [25]
Clofibric acid	308-328	10-22	25.7-85.6	Ming-Chen et al. [53]
Fenofibrate	308-328	10-22	183-666	Ming Chen et al. [53]
Gemfibrozil	308-328	10-22	83-419	Ming Chen et al. [53]
Chlorpheniramine maleate	308-338	16-40	0.154-4.26	Lashkarbolooki et al. [54]
Lovastatin	308-348	12.1-35.4	2.8-11.4	Hojjati etl al. [55]
Simvastatin	308-348	12.1-35.4	3-53.5	Hojjati etl al. [55]
Clozapine	318-348	12.1-35.4	0.36-4.19	Hosseini et al. [56]
Lamorigine	318-348	12.3-35.4	0.1-0.6	Hosseini et al. [56]

On the other hand, the dynamic method employs the usage of a continuous flow of one of the phases or the whole mixture through a bed of solute. Residence time must be long enough to allow thermodynamic equilibrium to occur. The dynamic method has the advantage of the ease of performing sampling, and it is faster than the static method though the probability of failure to reach equilibrium is the main drawback. A general schematic of the dynamic method is presented in **Figure 2-2**, it is worth mentioning that the experimental setup can be modified according to the investigated system.

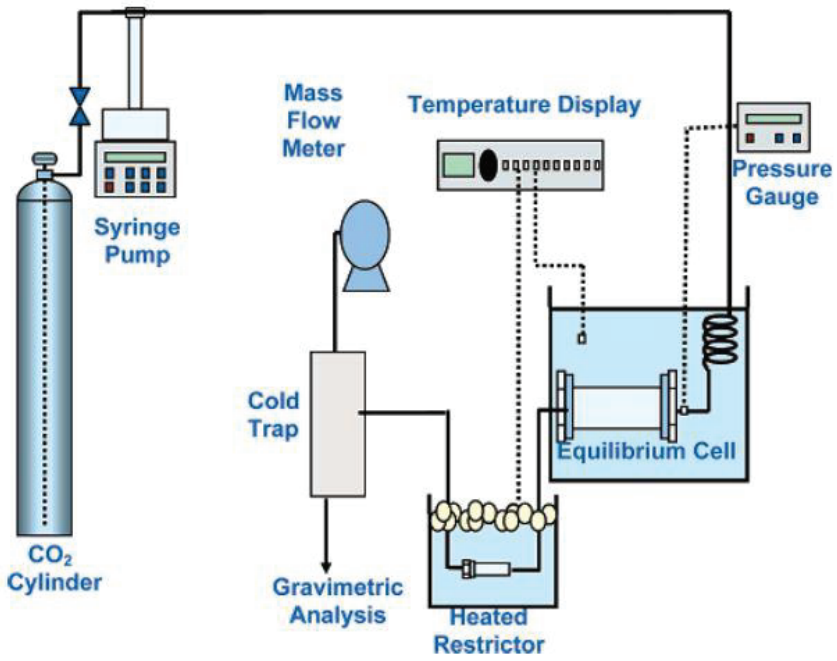

Figure 2-2. Schematic of the dynamic method for solubility measurements in $scCO_2$ [66]. Reprinted with permission from D. Suleiman et al.: *J. Chem.Eng. Data*. 50, 1234-1241 (2005) Copyright 2005 American Chemical Society.

Table 2-2 Examples for measuring the solubility of drugs by the dynamic method

API	Temperature [K]	Pressure [MPa]	Solubility $\times 10^5$	Authors
Cefuroxime axetil	308-328	8-25	0.02-1.24	Ongkasin et al. [57]
Isoniazid	308-313	13-18.5	12-40	Haryanto et al. [58]
Ketoprofen	313-328	9-25	0.39-9.15	Stassi et al. [59]
Ibuprofen	308-318	8-13	1.5-32	Ardjmand et al. [60]
Gemifloxacin	313-333	12-36	1.3-16	Shi et al. [61]
Enrofloxacin	313-333	12-36	0.6-56	Shi et al. [61]
Ciprofloxacin	313-333	12-36	0.2-1.8	Shi et al. [61]
Penicillin	313-333	10-35	0.53-6.3	Gordillo et al. [62]
Aspirin	308-328	10-25	8.9-34	Huang et al. [63]
Piroxicam	312-331	10-22	0.45-4.33	McNaughton et al. [64]
Nimesulide	312-331	10-22	1.89-9.85	McNaughton et al. [64]

The dynamic method was used to measure the solubility of different kinds of drugs at a wide range of temperatures and pressures as shown in **Table 2-2**. This method can be used with other compounds such as the measurement of food processing compound vanillic acid by Stassi et al. [59] , and the measurement of the solubility of vegetable oils by Sovova et al. [65]. The reliability and flexibility of the continuous flow method can be deduced from the various applications it is used in and the wide spectrum of operating conditions it is suitable for [66].

2.3. Thermodynamic modeling approaches

Despite the valuable efforts done toward the experimental measurement of the solubility of drugs in supercritical carbon dioxide, the knowledge we have is still limited. This can be attributed to the economic cost and time needed to carry out the necessary measurements for the APIs of interest owing to the complex instruments and methods required, the vast number of pharmaceutical compounds, and the wide range of operating conditions of temperature, pressure, and composition that can be used in the supercritical deposition process. It can be deduced that acquiring the needed knowledge for all those compounds through experimental data is most unlikely [67].

Though thermodynamic modeling is a promising tool for tackling experimental difficulties, there are challenges that need to be addressed. The promise of thermodynamic models is that they can enable us to correlate the existing solubility experimental data and predict or estimate solubilities beyond the measured range. However, drugs have complex chemical structures and different functional groups that complicate the task, also there is a lack of reliable thermodynamic models that can perform the required simulation work. In addition, the pure component materials of drugs are limited due to the previously mentioned experimental difficulties [8].

Thermodynamic modeling of the dissolution steps includes the usage of several approaches with each of them having its own strengths and shortcomings. However, three approaches are the most popular in the produced publications, which are modeling by Equations of state (EoS), semi-empirical equations, and solution models [68].

2.3.1. The equation of state (EoS) method

The equation of state (EoS) approach is regarded as the most suitable approach to model the supercritical fluid-drug system though it has its own limitations. This approach considers the supercritical phase as a high-pressure gas in equilibrium with the solid solute. It has predictive potential, can be used to correlate the experimental results over a wide spectrum of temperatures and pressures, and can be also modified according to the studied system making it a good fit for engineering applications [23]. However, this approach may require prior knowledge of some of the pure component properties of the system such as critical properties, acentric factors, and sublimation pressure which may not be available for APIs, and thus are estimated by methods that would introduce error into the calculations [69].

The EoS approach generally uses mixing rules to account for the non-ideality of the system, those rules use binary interaction parameters to adjust the co-volume and the energetic parameters, the most common mixing rules are the van der Waals one and two interaction parameters [70]. Different mixing rules were introduced to improve the accuracy of the results, with some of them employing up to three parameters. It is worth mentioning that systems that include solid materials require at least a two-parameter mixing rule to obtain reliable results. Those parameters are usually determined by curve fitting the experimental data of the binary systems further highlighting the semi-empirical nature of some of the equations of this approach.

This approach uses equations of different theoretical backgrounds including cubic equations of state such as Peng Robinson (PR), Soave-Redlich-Kwong (SRK), Valderrama-Patel-Teja (VRT), etc. besides other equations such as the virial equation of state, as well as

the Statistical Associating Fluid Theory (SAFT) and its variants.

Peng Robinson (PR) [71] and Soave-Redlich-Kwong (SRK) [72] equations of state are cubic equations of state that were based on van der Waals (vdW) EoS, both equations maintain the repulsive term of vdW equation but use different formulation for the attractive terms[73]. The mathematical formula for vdW and SRK and PR equations are shown in equations (2-1), (2-2), and (2-3) respectively:

$$P=\frac{RT}{v-b}-\frac{a(T)}{v^2} \tag{2-1}$$

$$P=\frac{RT}{v-b}-\frac{a(T)}{v(v+b)+b(v-b)} \tag{2-2}$$

$$P=\frac{RT}{v-b}-\frac{a(T)}{v(v+b)} \tag{2-3}$$

PR and SRK equations relate pressure (P), temperature (T), and molar volume (v), they utilize two parameters (a, b) to represent intermolecular forces and co-volume effects. These equations can be used to calculate fugacities which are then used to account for equilibria in the system across the different phases. Mixing rules are needed along with combining rules when these equations are applied to mixtures, and these rules play a significant role in the accuracy of the produced results and thus should be selected carefully. The van der Waals one and two-parameter mixing rules are expressed by equations (2-4) and (2-5), while the combining rules are represented in equations (2-6) and (2-7):

$$a = \sum_{i=1} \sum_{j=1} x_i x_j a_{ij} \quad (2\text{-}4)$$

$$b = \sum_{i=1} \sum_{j=1} x_i x_j b_{ij} \quad (2\text{-}5)$$

$$a_{ij} = \sqrt{a_i a_j}(1 - k_{ij}) \quad (2\text{-}6)$$

$$b_{ij} = \frac{b_i b_j}{2}(1 - l_{ij}) \quad (2\text{-}7)$$

Where a_{ij} and b_{ij} ($i = j$) are parameters corresponding to pure components, while a_{ij} and b_{ij} ($i \neq j$) are called the unlike-interaction parameters. k_{ij} and l_{ij} are fitting parameters called the binary interaction parameters.

The need for accurate models to correlate and predict thermodynamic properties and phase equilibria for chemical processes involving complex molecules and the considerable advances in applied statistical mechanics led to the development of a new family of EoS that are based on perturbation theory including Statistical associating fluid theory (SAFT) [73],[74]and its variants such as the variable range statistical associating fluid theory (SAFT-VR)[75], Perturbed Chain SAFT (PC-SAFT) [33], the perturbed-chain polar statistical associating fluid theory (PCP-SAFT)[76], etc. . While SAFT uses the hard-sphere fluid, PC-SAFT uses the hard chain reference fluid to represent chain formation in the reference fluid, and can be formulated as in the following equation:

$$a^{\text{res}} = a^{\text{hc}} + a^{\text{disp}} + a^{\text{assoc}} \quad (2\text{-}8)$$

Where a^{res}, a^{hc}, a^{disp}, and a^{assoc} represent the residual, hard chain, dispersion, and

association Helmholtz free energy terms.

Table 2-3. Results of correlation of the solubility of esomeprazole in $scCO_2$ [77]
Reprinted with permission from G. Sodeifian *et al*.: *J. Supercrit. Fluid.* 154, 104606 (2019)

Modeling	Temp. (K)	k_{12}	l_{12}	m_{12}	AARD	R_{adj}	F – value
Case 1 PR,vdW2	308.2	0.116	−0.113	–	5.40	0.982	69.0
	318.2	0.042	−0.297	–	7.60	0.961	31.1
	328.2	−0.027	−0.469	–	16.80	0.915	13.9
	338.2	−0.092	−0.632	–	11.31	0.906	12.5
	overall	$k_{12} = -2.226 + \frac{721.784}{T}$	$l_{12} = -5.957 + \frac{1800.994}{T}$		–		
Case 2 PR,Renon	308.2	0.037	−0.124	3.460E-01	16.43	0.791	3.8
	318.2	0.015	−0.138	3.461E-01	26.52	0.753	3.2
	328.2	−0.005	−0.150	3.461E-01	35.97	0.706	2.7
	338.2	−0.024	−0.162	3.461E-01	39.97	0.849	5.3
	overall	$k_{12} = -0.646 + \frac{210.346}{T}$	$l_{12} = -0549 + \frac{130.770}{T}$		$m_{12} = 0.347 - \frac{0.153}{T}$		
Case 3 SRK,vdW2	308.2	0.158	−0.082	–	4.53	0.987	92.6
	318.2	0.087	−0.265	–	7.75	0.954	26.4
	328.2	0.021	−0.437	–	18.03	0.903	12.0
	338.2	−0.042	−0.599	–	14.77	0.893	10.8
	overall	$k_{12} = -2.095 + \frac{694.316}{T}$	$l_{12} = -5.906 + \frac{1795.018}{T}$		–		
Case 4 SRK,Renon	308.2	0.050	−0.139	3.326E-01	13.06	0.872	6.3
	318.2	0.023	−0.158	3.327E-01	24.61	0.816	4.3
	328.2	−0.002	−0.175	3.327E-01	34.25	0.777	3.5
	338.2	−0.026	−0.191	3.327E-01	40.19	0.866	6.0
	overall	$k_{12} = -0.805 + \frac{263.468}{T}$	$l_{12} = -0.725 + \frac{180.355}{T}$		$m_{12} = 0.333618 - \frac{0.30753}{T}$		

The EoS method was employed by numerous scholars to calculate the solubility of APIs in $scCO_2$, one example is the study conducted by Sodeifian et al. [77] on NSAID esomeprazole at 10-27 MPa and 308-338K, where the solubility was correlated by PR and SRK EoS with vdW two-parameters and Renon mixing rules, it was found that both equations produced reliable results. Houssaindokht et al. [78] used PR, Pazuki, and modified PR EoS to calculate the solubility of the drugs methimazole, phenazopyridine, and propranolol in $scCO_2$ at 12.2-35.5 MPa and 308-348 K, Adachi-Sugie, vdW single and binary mixing rules were used to find that Pazuki EoS produced the most accurate fits when coupled with vdW binary mixing rules. Monir Anvari et al. [79] used SAFT-VR EOS to calculate the solubility

of solid substances including eight drugs such as ketoprofen, nimesulide, and methimazole in $scCO_2$ at 12-22 MPa and 308-338K with considerable success.

Table 2-4 Results of correlation of the solubility of phenazopyridine in $scCO_2$ by Cubic EoS [78] Reprinted with permission from M.R. Houssaindokht *et al.*: *J. Supercrit. Fluid.* 43, 390-397 (2008) Copyright 2008, Elsevier B.V. All rights reserved

	%AARD			k_{12}			l_{12}			λ_{12}		
	Mix 1	Mix 2	Mix 3	Mix 1	Mix 2	Mix 3	Mix 1	Mix 2	Mix 3	Mix 1	Mix 2	Mix 3
$T = 308$ K												
PR-EOS	23.62	14.46	13.06	1.18	0.37	0.36	–	−0.78	−0.79	–	–	−0.44
Pazuki-EOS	5.11	2.50	6.44	−0.37	0.04	0.03	–	−0.35	−0.33	–	–	0.05
MPR-EOS	19.29	14.21	12.81	1.27	0.31	0.30	–	−0.79	−0.82	–	–	0.49
$T = 318$ K												
PR-EOS	34.24	20.34	20.13	0.78	0.70	0.71	–	−0.80	−0.82	–	–	−0.03
Pazuki-EOS	4.78	2.02	4.78	−0.39	−0.12	−0.13	–	−0.53	−0.08	–	–	−0.26
MPR-EOS	25.59	18.43	18.32	1.23	0.79	0.78	–	−0.79	−0.81	–	–	0.01
$T = 328$ K												
PR-EOS	42.11	20.72	20.69	0.78	0.20	0.21	–	−0.80	−0.81	–	–	−0.80
Pazuki-EOS	9.80	3.41	3.34	−0.40	−0.07	−0.08	–	−0.68	−0.08	–	–	−0.18
MPR-EOS	29.10	20.88	23.10	0.83	0.27	0.26	–	−0.75	−0.78	–	–	−0.01
$T = 338$ K												
PR-EOS	35.38	23.08	22.71	0.41	−0.03	−0.02	–	−0.80	−0.82	–	–	−0.02
Pazuki-EOS	7.86	3.39	3.39	−0.32	−0.27	−0.30	–	−0.59	−0.58	–	–	−0.25
MPR-EOS	29.28	22.71	22.40	0.45	0.02	0.01	–	−0.80	−0.82	–	–	0.01
$T = 348$ K												
PR-EOS	34.18	17.78	17.41	0.70	−0.31	−0.30	–	−0.80	−0.82	–	–	−0.01
Pazuki-EOS	12.38	7.40	7.36	−0.23	−0.26	−0.28	–	−0.25	−0.26	–	–	0.02
MPR-EOS	38.82	18.46	18.45	−0.25	−0.36	−0.37	–	0.53	0.52	–	–	0.01

The EoS method can be used with ternary systems that use a co-solvent to increase the solubility of the API in $scCO_2$ with considerable success. Kikic et al. [80] used PR EoS coupled with vdW two-parameter mixing rule to estimate the isothermal solubility of acetaminophen, acyclovir, atenolol, carbamazepine, ibuprofen, naproxen, numesulide, and sotalol hydrochloride in mixtures of $scCO_2$ and organic solvents such as acetone, dimethyl sulfoxide, dichloromethane and ethanol at a wide range of pressure, it was concluded that PR EoS was able to describe the system satisfactorily. Ting et al.[81] investigated the effect of

six co-solvents Ethyl acetate, Acetone, Methanol, Ethanol, 1-propanol, and 2-propanol on the solubility of NSAID Naproxen in $scCO_2$ at 10-20 MPa and 313-331 K using PR and SRK EoS with vdW two-parameter mixing rules, both equations produced reliable results with SRK being the slightly superior model.

2.3.2. Semi-empirical equations method

The semi-empirical equations approach avoids some of the problems associated with the EoS approach, but it comes with drawbacks of its own. These equations are simple to use, don't require prior knowledge of the drug's physicochemical properties, and use easier to acquire values of the system pressure, temperature and the density of the supercritical fluid, this makes them easier to apply than the EoS approach. However, the main limitation of this approach is that knowledge of the experimental solubility data is essential to calculate the needed values for their adjustable variables limiting their predictive capabilities [82]. Furthermore, due to the wide variety of drugs and the different functional groups they possess, there is no definite semi-empirical equation that works with all drugs, and careful selection is needed [47]. Lastly, numerous researchers noted their accuracy decreases at elevated temperatures [58], [59]. Some of the most popular semi-empirical equations will be listed in the following section:

Chrastil equation is one of the most used semi-empirical equations, it is based on the similarity between the plot of reduced density vs reduced pressure of the supercritical fluid, and the plot of the solubility of the solid solute vs the reduced pressure of the solvent, at a temperature just above the critical temperature of the solvent [85]. The equation assumes

that each molecule of the solute associates with k molecules of the supercritical solvent to form a solvate complex that is in equilibrium with the system. Three variables (a_o, a_1 and a_2) are used in this equation to calculate solute solubility and are all determined by fitting to the experimental solubility data. The variable a_o is a function of the solute and solvent molecular weights, a_1 is related to the average number of solvent molecules in the complex and a_2 depends on the total heat. The Chrastil equation is formulated as follows:

$$\ln S = a_o + a_1 \ln \rho + \frac{a_2}{T} \qquad (2\text{-}9)$$

Where S is the molar solubility, ρ is the density of the SCF and T is the temperature.

Chrastil equation has some limitations such as unsuitability for usage over a wide range of temperature and the inability to produce accurate results when high concentrations of the solute are dealt with [86]. As a result, some modifications were introduced to the Chrastil equation such as the Adachi-Lu equation and Del Valle-Aguilera equation. Del-Valle and Aguilera [87] adjusted the Chrastil equation to account for the change in the vaporization enthalpy with temperature, where the modifications introduced by Adachi and Lu [88] formulated the association number K to be a function of temperature and pressure in contrary to Del-Valle and Aguilera who considered it as a constant number. The Del Valle-Aguilera and Adachi-Lu equations are formulated as in Equations. (2-10), and (2-11) respectively:

$$\ln y_2 = B_o + \left(B_1 + B_2\rho + B_3\rho^2\right) \ln\rho + \frac{B_4}{T} \qquad (2\text{-}10)$$

Where y_2 is the molar solubility, ρ is the density of the supercritical fluid and T is the

temperature, the equations have five table parameters (B_0, B_1, B_2, B_3, B_4) that need to be determined by curve-fitting.

$$\ln y_2 = D_0 + D_1 \ln\rho + \frac{D_2}{T} + \frac{D_3}{T^2} \quad (2\text{-}11)$$

Where y_2 is the molar solubility, ρ is the density of the supercritical fluid and T is the temperature, the equation has four table parameters (D_o, D_1, D_2, D_3) that need to be fitted.

Mendez-Santiago and Teja [89] suggested an equation that was based on the theory of dilute solutions, this equation uses the sublimation pressure of solute properties on the contrary of the Chrastil equation and its modifications that don't consider the solute properties. In their model, an enhancement factor (E) that depends on the solvent's density was introduced as well, the Mendez Santiago- Teja can be formulated as follows:

$$T \ln(E) = T \ln\left(\frac{y_2 P}{P_2^{sub}}\right) = a + b\rho \quad (2\text{-}12)$$

where T is the temperature in Kelvin, E is the enhancement factor, y_2 is the molar solubility of the solid solute, P is pressure of the system, P_2^{sub} is the sublimation pressure of the solute, and a and b are determined by fitting to the experimental data.

Bartle et al. [90] suggested a model that modifies the formulation of the enhancement factor and uses a reference pressure as a corrective term to limit the effect of experimental errors of the solubility data. Bartle equation also uses the critical density of the supercritical fluid as a reference density. The equation of the Bartle model is as follows:

$$\ln\left(\frac{y_2 P}{P_{ref}}\right) = a_0 + a_1\left(\rho - \rho_{ref}\right) + \frac{a_2}{T} \qquad (2\text{-}13)$$

Where y_2 is the molar solubility of the solid solute, P is the pressure of the system, P_{ref} is the reference pressure, ρ is the density of the supercritical fluid at the process conditions, ρ_{ref} is the reference supercritical fluid density, T is the temperature, and a_0, a_1, a_2 are adjustable parameters.

While these are some of the most popular semi-empirical equations, there are other equations that are used widely by researchers to calculate the solubility of solid solutes in supercritical fluids. Continuous modifications are introduced and some of the equations have up to six adjustable variables such as Garlapti-Madras and Yu equations. Other equations introduce different formulations of solubility and different mathematical expressions for the process variables such as the Sparks model which is necessarily a modification on the Adachi-Lu equation, Bian equation that employs produce five adjustable parameters and suggests a linear relationship between the logarithm of solubility and each of the logarithm of density of the supercritical fluid.

Table 2-5. Correlation of the solubility of aprepiant in $scCO_2$ using semi-empirical equations [94] Reprinted with permission from G. Sodefian *et al.*: *J. Supercrit. Fluid.* 128, 102-111 (2017) Copyright 2017, Elsevier B.V. All rights reserved

Model	a_0	a_1	a_2	a_3	a_4	a_5	AARD%	R_{adj}[b]	F-value[c]
Chrastil	6.60	−28.0	−5661.80	-	-	-	18.34	0.9522	101.10
K-J	2.8604	0.0073	−6195.67	-	-	-	15.04	0.9579	115.71
Bartle	18.80	0.0121	−8160.92	-	-	-	19.67	0.9438	63.96
Keshmiri	421.7188	−152669.0293	−0.0000735	−61.4324	21797.673	-	14.33	0.9799	145.33
Bian	4.1118	−0.0091	−25080.434	23.3404	30.6937	-	13.14	0.9868	223.34
Spark	−0.7734	2.9213	0.1152	9.6373	−21.4341	0.7147	14.24	0.9460	41.66

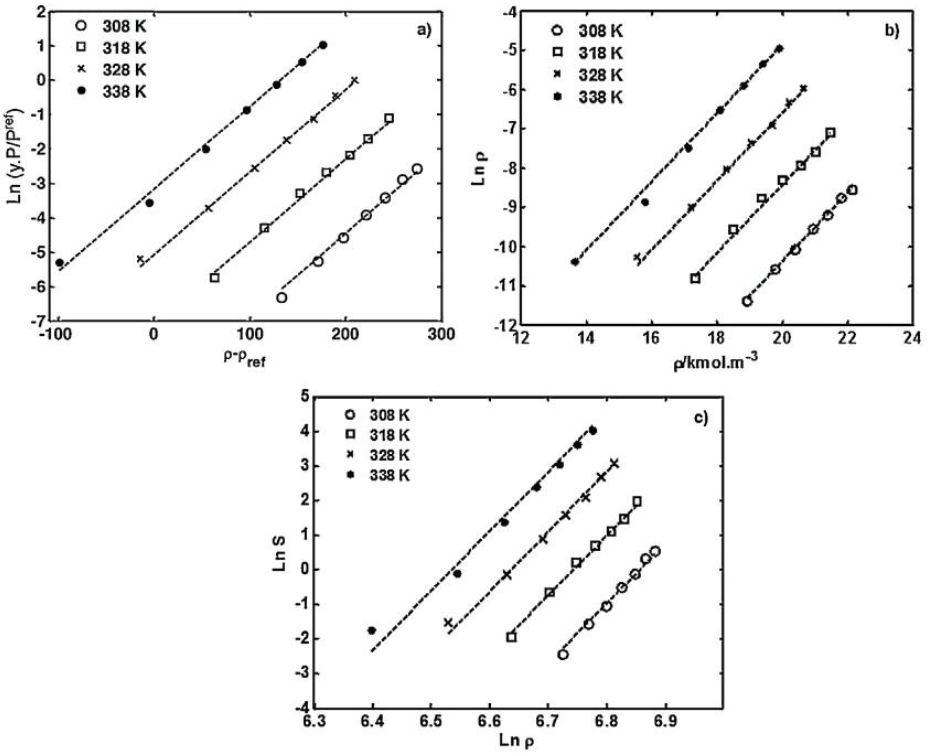

Figure 2-3. Correlation of solubility of piroxicam by semi-empirical equations: a)Bartle b)Kumar-Johnston c)Chrastil [90]. Reprinted with permission from S. Shojaee *et al.*: *J. Supercrit. Fluids* 81, 42-47 (2013) Copyright 2013, Elsevier B.V. All rights reserved

The semi-empirical equations are the most widely used models to correlate the solubility of solid solutes including APIs in supercritical fluids, they were used with systems of solid solute-supercritical fluid, solid solute–cosolvent–supercritical fluid and solid solute – co solute – supercritical fluid [91]. Banchero et al. [21] used 14 different semi-empirical models including Adachi-Lu, Kumar and Johnston, Chrastil, and Mendez Santiago – Teja to study the solubility of fenamate NSAIDs niflumic and tolfenamic acid at the pressure range 0f 16-40 MPa for the temperatures of 313-343K, the best results were obtained by Adachi-

Lu for niflumic acid, and by Del Valle-Aguilera equation for tolfenamic acid. Tabernero et al. studied the solubility of twenty-seven APIs using nine different semi-empirical models including Chrastil, Sparks, and Yu models at a wide range of temperatures and pressures, the study found that Sparks equation provided the best fit except when the data involved a wide range of temperature or pressure, in this case, the authors recommended Gordillo model [92]. Shojaee et al. [93] studied the solubility of NSAID piroxicam in $scCO_2$ at 16-40 MPa and 308-338 K using several semi-empirical models including Chrastil, Bartle, Kumar Johnston, and Mendez Santiago – Teja, all of these models produced results with the range of experimental error with Mendez Santiago – Teja slightly more accurate than the other three.

The semi-empirical equations approach was also used to study the solid solute–cosolvent–supercritical fluid with considerable success. Sodeifian et al. [94] used methanol as a co-solvent to improve the solubility of the *chemotherapy drug* aprepiant in $scCO_2$ at 15-33 MPa, and 308-338 K using five different models: Mendez Santiago – Teja, Jouyban, Gonzalez, Garlapti-Madras, and Reddy-Madras with the latter providing the best performance among the investigated systems. Huang et al. [63] used Chrastil and Kumar Johnston models to correlate the data of the aspirin-acetone- $scCO_2$ system at 10-25 MPa and 308-328K successfully with the Chrastil model proving superior

Studies of the solid solute – co-solute – Supercritical fluid system include the investigation done by Hosseini et al. [95] on the impact of adding menthol as a co-solute on the solubility of the *antipsychotic agent* clozapine and epilepsy drug lamorigine in $scCO_2$ at the pressure range of 12.3-33.7 MPa at 313-323K using five different models including Chrastil, Bartle, Kumar Johnston, Mendez Santiago–Teja and Thakur to find that Mendez

Santiago- Teja model produced the best results. Reddy et al. [96] studied the solubility of pharmaceutical agents: resorcinol and pyrocatechol mixtures in $scCO_2$ at 9.8-16.2 MPa and 308-338K with Mendez Santiago Teja model producing satisfactory results for the correlation of experimental data.

Table 2-6. Correlation of the solubility of resorcinol and pyrocatechol in $scCO_2$ using MST model [96].Reprinted with permission from S. Reddy *et al*.: *Thermochim. Acta* 521, 41-48 (2011) Copyright 2011, Elsevier B.V. All rights reserved

Solute		A/K	B/K mol^{-1} ml	C	AARD (%)
Resorcinol	Binary	−10,830	96,340	25.4	18.53
	Ternary	−10,550	116,500	23.04	21.81
Pyrocatechol	Binary	−10,390	114,500	24.73	18.55
	Ternary	−9424.3	99,170	22.61	23.78

As shown, the semi-empirical equations approach can correlate the solubility data of a wide selection of pharmaceutical materials at a spectrum of temperatures and pressures with considerable success. The careful selection of the model is fundamental in order to obtain the best fit at the used concentrations of the API and the operating conditions of the system.

2.3.3. Solution parameters model

The solution models combine some of the features of the EoS and semi-empirical equations as they possess a predictive potential, and their parameters can be generalized[47]. The solution model approach does not require the knowledge of critical properties or acentric factors like the Peng Robinson equation of state, it also has the flexibility of modifying its parameters to fit the different groups of pharmaceutical compounds. enhancing the prediction

accuracy [53].

The regular solution model views the supercritical phase as an expanded liquid solution in equilibrium with a solid solute. To express the non-ideal behaviour of the solute, the activity coefficient at infinite dilution is used, which is a sound assumption owing to the typically low concentrations of APIs in $scCO_2$. The solubility of the solid substance is calculated via the following equation:

$$y_2 = \frac{f_2^s}{\gamma_2^\infty f_2^l} \tag{2-14}$$

Where y_2 is the molar solubility of the solute, f_2^s and f_2^l are the fugacities of pure solute in the solid phase and supercritical phase, respectively, and γ_2^∞ is the activity coefficient of the solid solute at infinite dilution

The solution model is often incorporated with the Flory-Huggins equation, and the solubility of the solid solute in $scCO_2$ can be calculated as in Eq.(15):

$$\ln y_2 = \frac{\Delta H_2^{fus}}{R}\left(\frac{1}{T_{m,2}} - \frac{1}{T}\right) - \frac{V_2}{RT}(\delta_1 - \delta_2)^2 - 1 + \frac{V_1}{V_2} + ln\left(\frac{V_2}{V_1}\right) \tag{2-15}$$

where ΔH_2^{fus} is the enthalpy of fusion, R is the universal gas constant T is the absolute temperature, $T_{m,2}$ is the melting point of the solid, δ_1 is the solubility parameter of $scCO_2$, δ_2 is the solubility parameter of the solid component, V_1 is the molar volume of $scCO_2$ and V_2 is the molar volume of the solid solute.

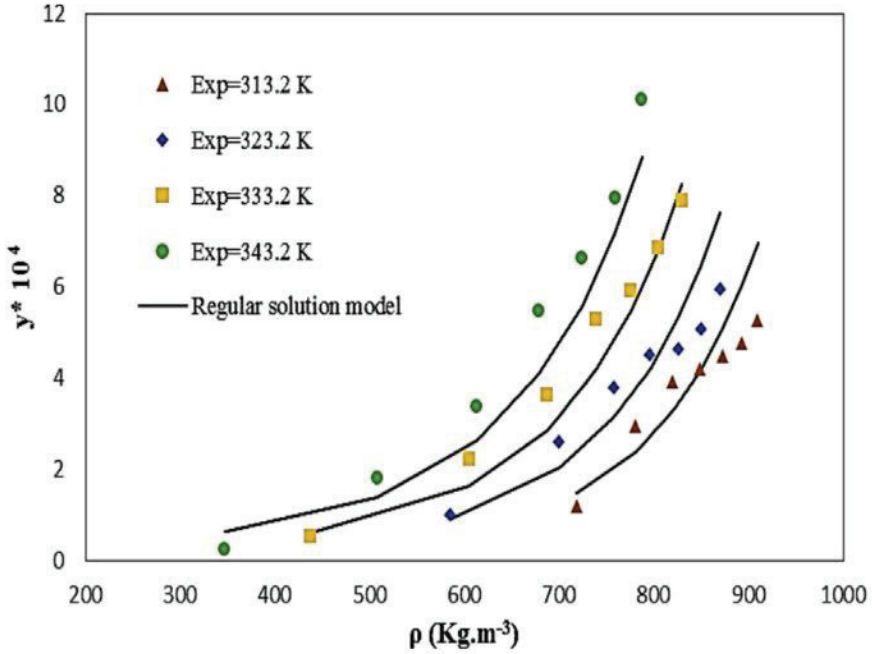

Figure 2-4. Correlating the solubility of Amiodarone Chloride using the solution model. Reprinted with permission from G. Sodeifian *et al*.: *J. Supercrit. Fluids* 450, 149- 159 (2017) Copyright 2017, Elsevier B.V. All rights reserved

The solution model approach was used by numerous scholars to calculate the solubility of multiple APIs in $scCO_2$ over a wide range of temperatures and pressure. Matsuyama et al. [97] studied the solubilities of *flavonoids* quercetin and 7,8-dihydroxyflavone at 308-318K and 9.1-25.3 MPa. Sodeifian et al. [82] calculated the solubility of *the antiarrhythmic drug* amiodarone hydrochloride at 12-30 MPa and 313.2-343.2K using the regular solution model with Flory-Huggins equation. Ming-Chen et al. [53] correlated the solubility of *antilipemic agents* of clofibric acid, fenofibrate, and gemfibrozil at 10-22 MPa and 308-318K with a satisfactory accuracy of 4-8%. Su et al. [98] investigated the solubility of NSAIDs nabumetone, phenylbutazone, and salicylamide at 10-22 MPa and 308-328K. One last example is the work of Cheng et al. [99]on the solubility of ketoprofen,

nifedipine, numesulide, and piroxicam at 10-29.6 MPa and 312.5-331.5K.

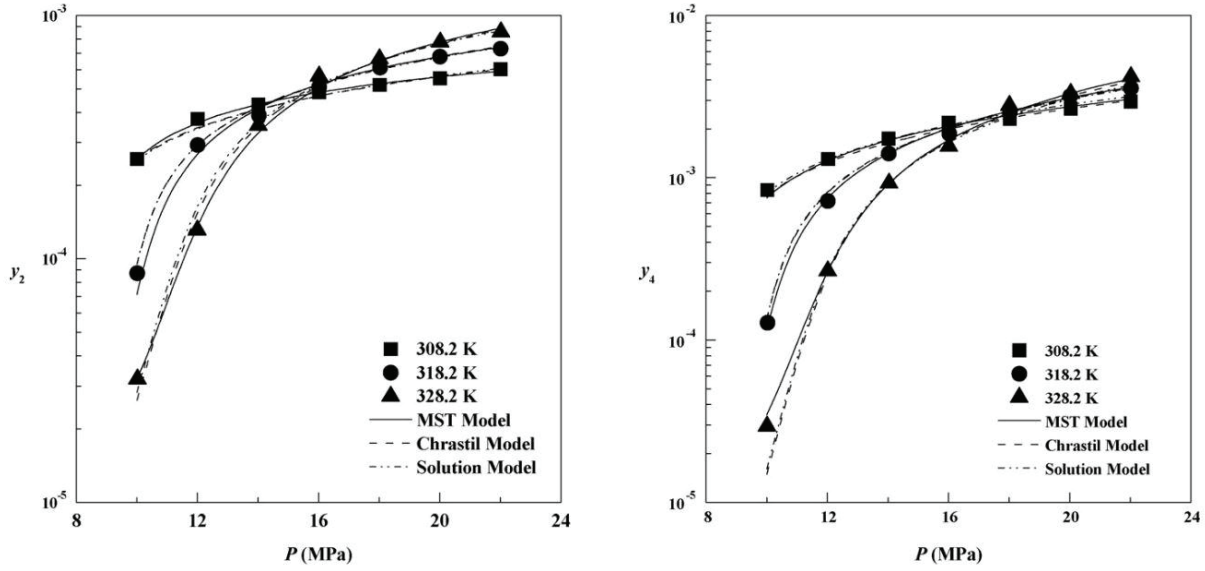

Figure 2-5. Correlation of the solubility of Clofibric acid(left) and Gemfibrozil (right) by the solution model [53].
Reprinted with permission from C. Yen-Ming *et al*.: *J. Supercrit. Fluids* 52, 175-182 (2010)

2.3.4. Comparison between the different thermodynamic approaches

As shown in the previous sections, it is not unusual for researchers to use different models from one of the previously mentioned approaches (EoS, semi-empirical density equations, and solution models) in a single study. In addition, some of the publications employed two or more of those approaches to correlate or predict solubility for the same drug(s) at the same operating conditions and produced results that give us an insight into the performance of these approaches side by side.

Sodeifian et al. [29] studied the solubility of the *anti-cancer drug* sorafenib tosylate

in $scCO_2$ at 10-27MPa and 308-338K where eight different semi-empirical equations including Chrastil, Bian, and Bartle models along PR and SRK EoS coupled with Wong-Sandler and vdW two-parameter mixing rules to find that SRK EoS coupled with Wong-Sandler mixing rules was superior to the other used models. In another study, Turk et al. [100] used a cubic EoS, PR coupled with vdW1 mixing rules, and a non-cubic EoS, Leonard-Kraska, along with two semi-empirical equations, Kumar Johnston, and Mendez Santiago – Teja to correlate the solubility of ibuprofen, salicylic acid, and naproxen in $scCO_2$ at 8-35 MPa and 308-353 K, the study showed that the semi-empirical equations produced more accurate results than the two EoS used with Mendez Santiago – Teja equation coming on top.

Su et al. [98]used the regular solution model coupled with the Flory-Huggins equation to correlate the solubility of 10 pharmaceutical compounds in $scCO_2$, and then compared its results with those produced by Chrastil and Mendez Santiago – Teja to find that though the semi-empirical equations were more accurate, the solution model using less adjustable parameters produced comparable results. El-Hadj et al. [101] coupled PR, SRK EoS with vdW one and two-parameter mixing rules and then compared them to PC-SAFT EoS coupled with one-parameter mixing rule to correlate the solubility of *NSAIDS* nabumetone, phenylbutazone and salicylamide) and *statin drugs* fluvastatin, aorvastatin, lovastatin, simvastatin, and rosuvastatin at 10-36 MPa and 308-348K, it was found that PC-SAFT produced better results than the cubic EoS.

It can be deduced that no approach proved to be superior for all the APIs investigated so far. That can be attributed to the vast number of pharmaceutical compounds and their complex structure, and the wide range of used operating conditions. It was found that the

proper selection of the mixing rules employed with the EoS, the choice of the semi-empirical model to be used, and the value of some of the solid solute pure component properties especially the sublimation pressure can play a significant part in the accuracy of the produced results.

Chapter 3 : Methodology

In this chapter, the methodology used to conduct this study will explained in detail. First, the materials used in the study will be presented and their properties will be listed. Next, the details of the experimental setup used to measure the solubility of the investigated drugs in $scCO_2$ will be introduced. Lastly, the thermodynamic model will be explained, and the relevant equations will be stated

3.1. Materials

Three non-steroidal anti-inflammatory drugs (NSAIDs) were chosen as the focus of

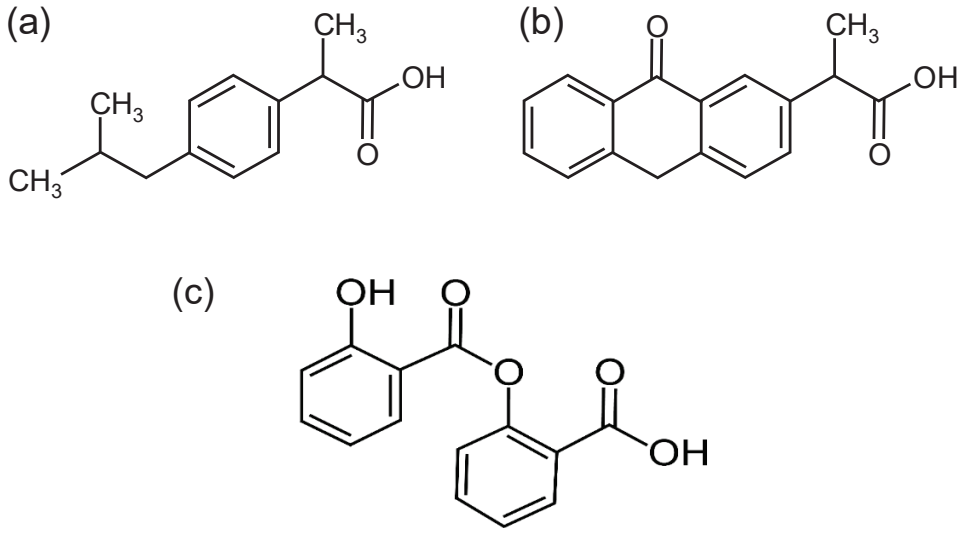

Figure 3-1. The structural formula of the used APIs: a) Ibuprofen, b) Ketoprofen, c) Salsalate.

this study: ibuprofen, ketoprofen, and salsalate. These three drugs were chosen as they are model drugs that are widely used by scholars facilitating the evaluation and assessment of the obtained results in this investigation, and due to their reliable solubility data in $scCO_2$

over a spectrum of pressure and temperature (published by Charoenchaitrakool et al. [102] for ibuprofen, by Sabegh et al. [67], McNaughton et al. [64] for ketoprofen, and by Zabihi et al.[103] for salsalate) and due to their availability.

Ibuprofen (**Figure 3-1(a),** IUPAC name: 2- [4-(2-methyl propyl) phenyl] propanoic acid) is a class II drug of the pharmaceutical classification system, that is derived from propionic acid [104], [105]. It has analgesic and antipyretic without producing addiction and is widely used for all symptoms related to acute or chronic pain. ibuprofen has limited oral bioavailability due to its low dissolution rate [87].

Ketoprofen (**Figure 3-1(b),** IUPAC name: 2-(3-benzoyl phenyl) propanoic acid) is a non-steroidal anti-inflammatory drug (NSAID) that was first manufactured by Rhone-Poulenc research laboratories in Paris in 1967 [106]. It is used widely as an analgesic and antipyretic and is prescribed to relieve pain, to reduce swelling and joint stiffness. It is important to mention that ketoprofen produces fewer side effects if compared with other NSAIDs and hence its presence in pharmaceutics has gained more prominence [107]

Salsalate (**Figure 3-1(c),** IUPAC name: 2-(2-hydroxybenzoyl) oxybenzoic acid) is a non-steroidal anti-inflammatory drug (NSAID) in a group of drugs called salicylates .it is used to relieve pain from various conditions, reduce, swelling, and joint stiffness due to arthritis, and it can be used to treat diabetes [108].

In this study, several organic solvents were chosen to determine the PC-SAFT pure components parameters for the investigated APIs as previously explained in **Chapter 1**. The chosen solvents have different functional groups and have reliable data in the literature that involves a wide range of temperatures and an adequate number of data points to facilitate the

evaluation of the produced experimental results, also the selected solvents don't form hydrogen bonds to comply with the assumptions of this study. These solvents are chloroform (a halogen), acetone (a ketone), ethyl acetate (an ester), toluene (an aromatic), and o-xylene (an aromatic). The solubility values of ibuprofen in organic solvents were obtained from the literature [109], [110], and the solubility data of ketoprofen in organic acetone, toluene, and o-xylene was measured in this study, but its solubility in ethyl acetate was obtained from the literature[111], and lastly, the solubility of salsalate was measured in this study. The CAS numbers, suppliers, and purities of the used materials are listed in **Table 3-1**. All APIs targeted in this work are racemic.

Table 3-1. Supplier, CAS number, and purity of the used chemicals for measuring APIs solubilities in organic solvents in this study.

Chemicals	CAS Number	Supplier	Purity [mass%]	Purification method
Ketoprofen	22071-15-4	Tokyo Chemical Industry	98.0	none
Salsalate	552-94-3	Tokyo Chemical Industry	98.0	none
Toluene	108-88-3	Nacalai Tesque	99.8	none
o-Xylene	95-47-6	Nacalai Tesque	99.8	none
Acetone	67-64-1	Nacalai Tesque	99.5	none
Ethyl acetate	141-78-6	Nacalai Tesque	99.8	none

3.2. Experimental setup

The solubility measurements for ketoprofen and salsalate in selected solvents were performed at atmospheric pressure by the static method, based on the routine adopted by Paus et al.[39]. An excess amount of the APIs was added to each of the studied organic solvents in an elementary flask of 200 cm^3 volume. A magnetic stirrer (ThermoScientific, USA) was used to mix the solution at 500 rpm, and the temperature was controlled by a water bath (EYELA, Japan, SBC-16). A calibrated platinum resistance thermometer was used to measure the temperature of the system with an accuracy better than ± 0.1K. The used Erlenmeyer flasks that contained the solution were capped by a rubber stopper with a hole of c.a. 3mm, and the effect of the water from the atmosphere on the measured solubility was neglected due to the organic solvent-generated vapor pressure.

The system was kept at a uniform temperature for at least 24 hours to guarantee the achievement of equilibrium, the magnetic stirrer was stopped for at least half an hour and then a small sample of the supernatant solution was taken and diluted.

Next, the concentration of the API in the sample was measured by a UV-vis spectrometer (U-3900H, Hitachi High- Tech Corp., Japan) at a wavelength of 330 nm based on pre-prepared calibration curves (the coefficient of determination (R^2) was higher than 0.9995).

Due to the difficulty of measuring the mass of the dissolved API with the needed accuracy because of its low solubility, UV-vis absorbance analytical method was chosen ahead of a mass-based solubility measurement. The following equation for the temperature

dependence of the solvent density for a saturated liquid was used to convert the concentration of the dissolved API from mass to molar concentration.

$$d_s(T) = \frac{A}{B\left\{1+\left(1-T/C\right)^D\right\}} \tag{3-1}$$

Where $d_s(T)$ is the solvent density (g/dm^3) at the temperature T (K), and A, B, C, and D are model parameters obtained from the literature[112], [113]

The solution density was considered to be equal to the pure solvent density due to the low solubility of the API in the solvent, then the mole fraction of the API in the solution could be calculated using the following equation:

$$x^{API} = \frac{\frac{c_{API}}{M_{API}}}{\frac{c_{API}}{M_{API}} + \frac{d_s(T)}{M_s}} \tag{3-2}$$

where c_{API} is the measured metal precursor concentration in the solvents (g/dm^3), and M_{API} and M_s are the molar masses of the API and organic solvent, respectively.

The solubility of APIs in organic solvents (x_{API}) were measured at 278-306 K, which is less than the boiling temperature of the used solvents. Measurements were repeated at least twice for each data point, and their average was presented. The estimated value of $U_r(x_{API})$, the relative combined expanded uncertainty, was less than 0.05, with a confidence level of 0.95. The measured solubility values were found to be in good agreement with the literature data.

3.3. Model

The modeling approach in this study uses the Perturbed Chain Statistical Associating Fluid Theory (PC-SAFT) equation of state to estimate and correlate the solubility of the investigated APIs in both organic solvents and $scCO_2$. PC-SAFT was derived from the SAFT equation of state [33][32], and it combines perturbation theory and molecular thermodynamics [114]–[117]. PC-SAFT possesses some attractive features owing to its solid theoretical background such as the possibility of being validated against the results of molecular simulations, and its flexibility as its terms can be adjusted according to the investigated system to obtain more accurate results. Additionally, the clear physical meaning of the parameters of PC-SAFT makes it easier to derive new ones based on the existing ones easier [118].

Though it requires the sublimation pressure value of the APIs, PC-SAFT does not need some properties that are hard to measure experimentally such as critical properties or acentric factor that is required by cubic EoS, and that makes them unsuitable for estimating the solubilities of pharmaceutical agents in $scCO_2$. As a result, PC-SAFT was employed in several engineering applications including polymer systems[35], ionic liquids [119], the petroleum industry [120], and biofuels [121].

When components that associate via hydrogen bonds are not present in the studied system, PC-SAFT requires the knowledge of the values of three pure parameters (segment diameter σ_i, segment number m_i, and dispersion energy u_i) for each component i in the studied system to produce reliable results. These parameters are typically determined by fitting saturated liquid density and vapor pressure experimental data [38]. Even though this

method was used to measure the PC-SAFT pure parameters for several compounds such as CO_2 [33] ,using this method for APIs is challenging because many of them decompose at high temperatures.

A potential solution for this issue is the method reported by Paus et al. [39], where the PC-SAFT pure component parameters of various solid APIs such as itraconazole and griseofulvin were determined by using their solubility in organic solvents and then these values were employed to calculate their solubility in water. The usage of this approach, however, to calculate the solubility of solid APIs in $scCO_2$ has not been evaluated to date.

The modeling approach in this study consists of two steps; the first is the determination of PC-SAFT pure component parameters for the studied APIs via their solubility data in organic solvents. Next, those parameters will be used to correlate and estimate the solubility of the selected APIs in $scCO_2$. The contribution of molecular association was not considered due to the absence of hydrogen-bonding sites in the used organic solvents, and that the solubility of APIs in $scCO_2$ is minimal (their mole fraction is less than 0.01) limiting the effect of self-association (although this assumption should be revisited in future research). Therefore, the PC-SAFT equation used in this study can be expressed as in the following equation:

$$a^{res} = a^{hc} + a^{disp} \tag{3-3}$$

Where the detailed mathematical formula of the terms of the previous equation can be found in the Gross and Sadowski publication [33].

To model the binary systems, the Lorentz–Berthelot combining rules were used in this

work according to the following equations:

$$\sigma_{ij} = \frac{1}{2}\left(\sigma_i + \sigma_j\right) \tag{3-4}$$

$$u_{ij} = \left(1 - k_{ij}\right)\sqrt{u_i u_j} \tag{3-5}$$

The binary interaction parameter (k_{ij}) expresses the interactions between components, *i* and *j* of the system, and can be utilized as an adjustable parameter to improve the model accuracy if needed.

3.3.1. Determining the PC-SAFT parameters for the studied APIs

In this step, the experimental solubility of the investigated drugs in organic solvents was used to determine the three PC-SAFT pure component parameters, the values of those parameters for the used organic solvents and for $scCO_2$ can be found in the following table:

Table 3-2. PC-SAFT pure component parameters and molar mass for the used solvents

Component	M_i [g/mol]	m_i [-]	σ_i [Å]	u_i/k_B [K]	Reference
Acetone	58.079	2.8913	3.2279	247.42	[122]
Ethyl acetate	88.106	3.5375	3.3079	230.80	[33]
Toluene	92.141	2.8149	3.7169	285.69	[33]
o-Xylene	106.167	3.1362	3.7600	291.05	[33]
Chloroform	119.378	2.6060	3.4085	265.94	[123]
CO_2	44.010	2.6027	2.555	151.04	[38]

The condition of achieving equilibria in the API- organic solvent system is that the chemical potential of the API in the solid phase is equal to the chemical potential of the API in the liquid phase. Therefore, the solubility of each of the studied API in the liquid phase can be calculated by the following equation:

$$x_{\mathrm{API}} = \frac{1}{\gamma_{\mathrm{API}}} \exp\left\{ -\frac{\Delta h_{\mathrm{API}}^{\mathrm{fus}}}{RT}\left(1 - \frac{T}{T_{\mathrm{m}}}\right)\right\} \tag{3-6}$$

where γ_{API} is the activity coefficient of the API in the organic solvent, $\Delta h_{\mathrm{API}}^{\mathrm{fus}}$ is the heat of fusion the API, and T_{m} is its melting point; these parameters were obtained from the literature and are listed in (**Table 3-3**). Eq. (3-6) is commonly used to calculate the drug solubilities in organic solvents [124] [15]

Table 3-3. Some of the pure component properties for the investigated APIs

API	$\Delta h_{\mathrm{API}}^{\mathrm{fus}}$ [kJ/mol]	T_{m} [K]	$v_{\mathrm{API}}^{\mathrm{solid}}$ [cm^3/mol]
Ibuprofen	25.5[110]	347.15[110]	182.14[102]
Ketoprofen	37.3[125]	367.95[125]	195.6[59]
Salsalate	29.0[126]	430.2[126]	184.45[127]

The activity coefficient [30], [113] in Eq. (3-6) can be determined by dividing the fugacity coefficient of the solid API in the solvent ($\varphi_{\mathrm{API}}^{\mathrm{L}}$) and the fugacity coefficient of the pure API in liquid form ($\varphi_{0,\,\mathrm{API}}^{\mathrm{L}} = \varphi_{\mathrm{API}}^{\mathrm{L}}\left(x_{\mathrm{API}} \to 1\right)$) as in the next equation

$$\gamma_{\mathrm{API}} = \frac{\varphi_{\mathrm{API}}^{\mathrm{L}}}{\varphi_{0,\,\mathrm{API}}^{\mathrm{L}}} \tag{3-7}$$

These fugacity coefficients in turn can be calculated using the corresponding residual chemical potential as per the equation:

$$\ln\varphi_{\mathrm{API}} = \frac{\mu_{\mathrm{API}}^{\mathrm{res}}\left(V, T, x_{\mathrm{API}}\right)}{RT} - \ln Z \tag{3-8}$$

where the chemical potential ($\mu_{\mathrm{API}}^{\mathrm{res}}$) was determined from PC-SAFT via the following

equation:

$$\frac{\mu_{\mathrm{API}}^{\mathrm{res}}\left(T,V,x_{\mathrm{API}}\right)}{RT}=\frac{a^{\mathrm{res}}}{RT}+(Z-1)+\left(\frac{\partial\left(a^{\mathrm{res}}/RT\right)}{\partial x_{\mathrm{API}}}\right)_{T,V,x_{j\neq\mathrm{API}}}-\sum_{k=1}^{N}\left(x_k\left(\frac{\partial\left(a^{\mathrm{res}}/RT\right)}{\partial x_k}\right)_{T,V,x_{i\neq k}}\right) \tag{3-9}$$

The detailed equations of a^{res} and Z can be found in the publication by Sadowski and Gross [33].

When the values of the pure component parameters of the studied APIs were determined, the k_{ij} value in Eq. (3-5) was set to zero. A simplex optimization method in MATLAB® R2021a software was chosen to perform the fitting calculations for this study.

$$\mathrm{ARD}[\%]=\frac{1}{ND}\sum_{i}^{ND}\frac{\left|x_{\mathrm{API,calc},i}-x_{\mathrm{API,exp},i}\right|}{x_{\mathrm{API,exp},i}}\times 100 \tag{3-10}$$

3.3.2. Estimating and correlating the solubility of APIs in $scCO_2$

In this step, the solubility values for the studied APIs in $scCO_2$ was both estimated and correlated using the pure component parameters calculated in the previous step. The equilibrium condition for the API-$scCO_2$ system is that the fugacity of the API is equal in both solid and supercritical phases. Thus, the solubility of the APIs in $scCO_2$ was calculated using the following equation

$$y_{\mathrm{API}}=\frac{p_{\mathrm{API}}^{\mathrm{sub}}}{P\varphi_{\mathrm{API}}^{\mathrm{scf}}}\exp\left[\frac{v_{\mathrm{API}}^{\mathrm{solid}}\left(P-p_{\mathrm{API}}^{\mathrm{sub}}\right)}{RT}\right] \tag{3-11}$$

where $v_{\mathrm{API}}^{\mathrm{solid}}$ is the API solid molar volume, $\varphi_{\mathrm{API}}^{\mathrm{scf}}$ is the fugacity coefficient of the API in the supercritical phase, which was calculated through Eqs. (3-6) and (3-7). The Clausius–

Clapeyron equation [128] was utilized to calculate the p_{API}^{sub} values (the sublimation pressure of the API) in Eq. (3-11) via the interpolation and extrapolation of the literature data listed in Table 3-4 according to the following mathematical formula

$$p_{API}^{sub} = p_{API}^{sub*} \exp\left[-\frac{\Delta h_{API}^{sub}}{R}\left(\frac{1}{T}-\frac{1}{T^*}\right)\right] \quad (3\text{-}12)$$

where Δh_{API}^{sub} is the sublimation enthalpy of the API, and T^* and p_{API}^{sub*} are the reference temperature and pressure, respectively.

Table 3-4. Values of the heat of sublimation, the reference sublimation pressure and the corresponding reference temperature for the studies APIs

APIs	Δh_{API}^{sub} [kJ/mol]	p_{API}^{sub*} [Pa]	T^* [K]	Reference
Ibuprofen	95.45	4.95×10^{-2} [a]	308.15 [a]	[102]
Ketoprofen	110.1	5.34×10^{-4} [b]	313 [b]	[59], [129]
Salsalate	140.5	9.09×10^{-2} [c]	336.8 [c]	[127]

a: Determined with a group contribution method [102], [130]
b: Determined with a modified Clausius–Clapeyron equation [59], [128]
c: Determined in this work based on the method proposed by Eusebio and Rojas[131]

The procedure to predict the API solubility in $scCO_2$ can be summarized as follows:

(i) The solubility of the target API in organic solvents was obtained by the means of experimental work or taken from literature

(ii) the APIs three pure component PC-SAFT parameters via fitting the solubility data of them in organic solvents.

(iii) The solubility of the APIs in $scCO_2$ was estimated using PC-SAFT EoS using the obtained pure components parameters in step (ii) with k_{ij} in Eq. (3-5) set to zero and was correlated after then using k_{ij} as an adjustable parameter

Chapter 4 : Results of the used experiments and thermodynamic model

In this chapter, the experimental and thermodynamic modeling results of the three investigated APIs will be presented. Firstly, their solubility in organic solvents will be measured and then used to determine the PC-SAFT pure component parameters. After then, these parameters will be used to estimate and correlate solubility in $scCO_2$.

4.1. Measurement and fitting drug solubility in organic solvents

4.1.1. Measurements results of drug solubility in organic solvents

The solubility data of ibuprofen in organic solvents was measured in the literature in different organic solvents at different temperatures, with and without co-solvents [4], [105], [109], [110], [124], [132]–[143][143]The data published by Gracin et al. [110] and Wang et al. [109] were chosen in this study due to their reliability, the number of data points provided, and the adequate range of temperatures investigated, the used values can be found in **Table 4-1.**

The solubility of ketoprofen in three solvents (toluene, o-xylene, and acetone), and the solubility of salsalate in four organic solvents (toluene, o-xylene, acetone, and ethyl acetate) were measured experimentally in this work, and the solubility of ketoprofen in ethyl acetate was taken from Soto et al. [111] which gave reliable data and used adequate number of data points. as. The used data for ketoprofen and salsalate are listed in **Table 4-2** and **Table 4-3** respectively.

Table 4-1. The used solubilities for ibuprofen in organic solvents

Solvent	T [K]	x [-]
Acetone [a]	283.57	0.1437
	288.49	0.1684
	293.37	0.1996
	297.87	0.2330
	303.25	0.2732
	308.07	0.3114
	312.65	0.3516
Ethyl Acetate [b]	283.17	0.1267
	288.47	0.1584
	293.57	0.1935
	297.69	0.2254
	302.75	0.2713
	307.83	0.3195
	313.07	0.3762
	318.45	0.4388
Toluene [a]	283.15	0.1034
	288.15	0.1329
	293.15	0.1696
	303.15	0.2509
	308.15	0.2995
Chloroform [b]	283.15	0.2093
	288.15	0.2429
	293.15	0.2718

a: Data published by Gracin et al. [110]
b: Data published by Wang et al. [109]

Table 4-2 The used solubilities of Ketoprofen in organic solvents

Solvent	T [K]	x [-]
Acetone [a]	279.55	0.0728
	284.30	0.0811
	288.35	0.0885
	293.2	0.0983
	297.65	0.1093
	302.85	0.1193
	279.55	0.0728
Ethyl Acetate [b]	278.15	0.1267
	283.15	0.1584
	288.15	0.1935
	293.15	0.2254
	298.15	0.2713
	303.15	0.3195
Toluene [a]	279.65	0.0084
	284.28	0.0105
	288.82	0.0138
	293.55	0.0194
	297.65	0.0241
	302.62	0.0341
o-Xylene [a]	279.4	0.0058
	284.1	0.0078
	288.8	0.0110
	293.4	0.0147

a: measured in this work
b: From the publication of Soto et al. [111]

Table 4-3. The used solubilities for salsalate in organic solvents

Solvent	*T* [K]	*x* [-]
Acetone [a]	280.15	0.074
	284.45	0.076
	289.05	0.081
	293.5	0.087
	298.1	0.091
	305.9	0.096
Ethyl Acetate [a]	279.8	0.053
	284.6	0.056
	288.95	0.06
	293.65	0.063
	297.65	0.067
	304.05	0.072
Toluene [a]	280.05	0.0014
	284.25	0.0018
	288.95	0.0025
	293.8	0.0026
	297.7	0.0031
	304.8	0.0046
o-Xylene [a]	279.7	0.0017
	284.1	0.0019
	288.8	0.0025
	293.4	0.0030
	297.9	0.0036
	302.9	0.0045

a: measured in this work

The solubility order of ibuprofen in the used solvents was chloroform > acetone ~= ethyl acetate > toluene, while the solubility order of ketoprofen and salsalate in the used solvents was acetone > ethyl acetate > toluene ~= o-xylene.

4.1.2. Fitting drug solubility in organic solvents using the PC-SAFT pure components parameters

The solubility values of ibuprofen, ketoprofen, and salsalate in the investigated solvents were fitted using the PC-SAFT equation of state. The binary interaction parameter (k_{ij}) was set to zero as PC-SAFT pure component parameters were determined for each of the investigated APIs. The obtained solubilities followed the established trend in literature, where the solubility of solid solutes in organic solvents increases with the increase in temperature confirming the validity of the obtained values.

The dashed lines in **Figure 4-1**, **Figure 4-2** and **Figure 4-3** express the produced solubility values for ibuprofen, ketoprofen, and salsalate respectively. **Table 4-4** list the average relative deviation (ARD) values between the experimental and calculated values for each of the ibuprofen–organic solvents system, while **Table 4-5** and **Table 4-6** list those values for ketoprofen and salsalate respectively. Lastly, the determined values for PC-SAFT pure components parameter for each of the investigated APIs and their molar mass are summarized in **Table 4-7**.

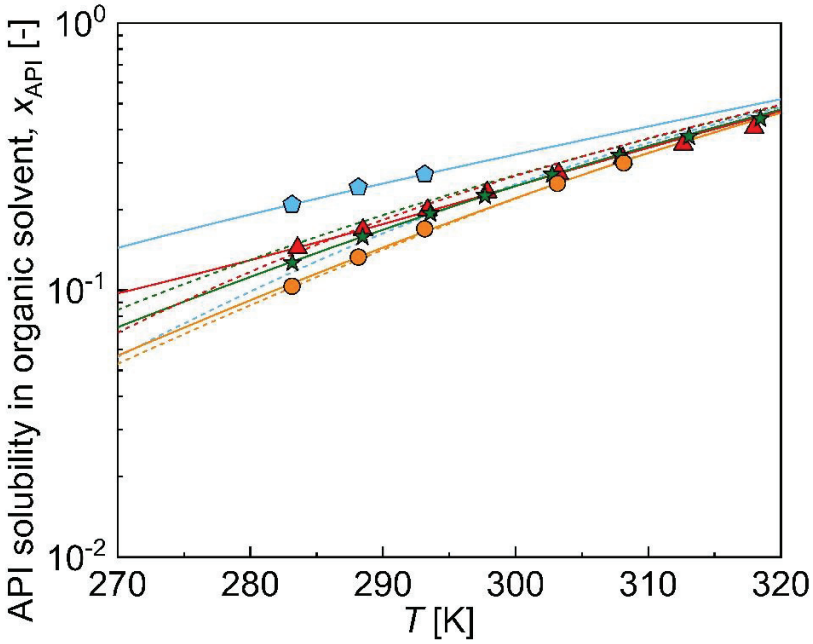

Figure 4-1. Solubility data of ibuprofen in organic solvents in chloroform (⬟,[110]), acetone (▲,[109), ethyl acetate (★,[109], and Toluene (●,[110]). The dashed lines are the fits calculated using PC-SAFT, at k_{ij} =0, with the pure-component parameters of ibuprofen used as adjustable parameters, the solid lines express the fits acquired when k_{ij} is used an additional adjustable parameter. The ideal solubility of API for γ_{API} =1 in Eq. (3-6) is illustrated as a dotted line.

Table 4-4. ARDs between the experimental and calculated solubility values by PC-SAFT, and kij (binary interaction parameter) in Eq. (3-5).

Solvent	Reference for solubility data	ARD (k_{ij}=0) [%][a]	$k_{ij,\text{slope}} \times 10^4$ [K^{-1}][b]	$k_{ij,\text{intercept}}$ [-][b]	ARD (with k_{ij}) [%][c]
Toluene	[110]	1.9	0.366	−0.0112	1.3
Ethyl acetate	[109]	10.6	0.857	−0.0199	0.9
Acetone	[110]	8.5	4.537	−0.1300	2.6
Chloroform	[109]	37.9	0.187	−0.0303	0.5
Overall		11.5			1.5

a: Average relative deviation for each solvent calculated using Eq. (3-10) by fitting the results produced by PC-SAFT with k_{ij} in Eq. (3-5) set to zero.
b: Parameters in Eq. (4-1).
c: ARD of the additional fitting using k_{ij} in Eq. (3-5).

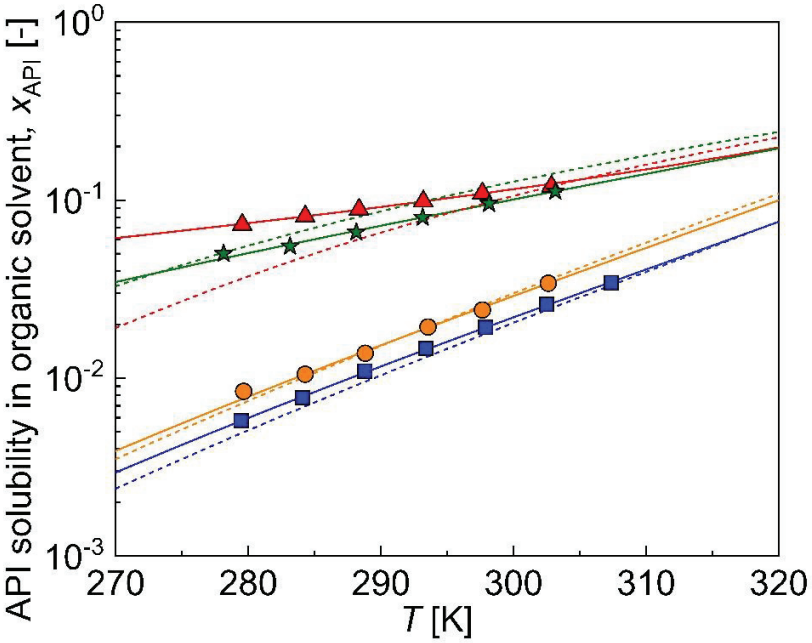

Figure 4-2. Solubility data of ketoprofen in organic solvents, acetone (▲: this study), ethyl acetate (★,[111, toluene (●: this study), and o-xylene (■: this study). The dashed lines are the fits calculated using PC-SAFT with the pure-component parameters of Ibuprofen as adjustable parameters at k_{ij} =0, and solid lines express the fits acquired when k_{ij} is used as an additional adjustable parameter. The ideal solubility if API for γ_{API} =1 in Eq. (3-6) is illustrated as a dotted line

Table 4-5. ARDs between the experimental and calculated solubility values by PC-SAFT, and kij (binary interaction parameter) in Eq. (3-5).

Solvent	Reference solubility data	forARD (k_{ij}=0) [%][a]	$k_{ij,slope} \times 10^4$ [K^{-1}][b]	$k_{ij,intercept}$ [-][b]	ARD (with k_{ij}) [%][c]
Toluene	This work	4.9	0.937	−0.0273	3.2
Ethyl acetate	[111]	18.8	4.276	−0.1168	1.8
Acetone	This work	26.2	8.801	−0.2685	0.9
o-Xylene	This work	9.8	0.801	−0.0256	0.9
Overall		14.7			1.5

a: Average relative deviation for each solvent calculated using Eq. (3-10) by fitting the results produced by PC-SAFT with k_{ij} in Eq. (3-5) set to zero.
b: Parameters in Eq. (4-1).
c: ARD of the additional fitting using k_{ij} in Eq. (3-5).

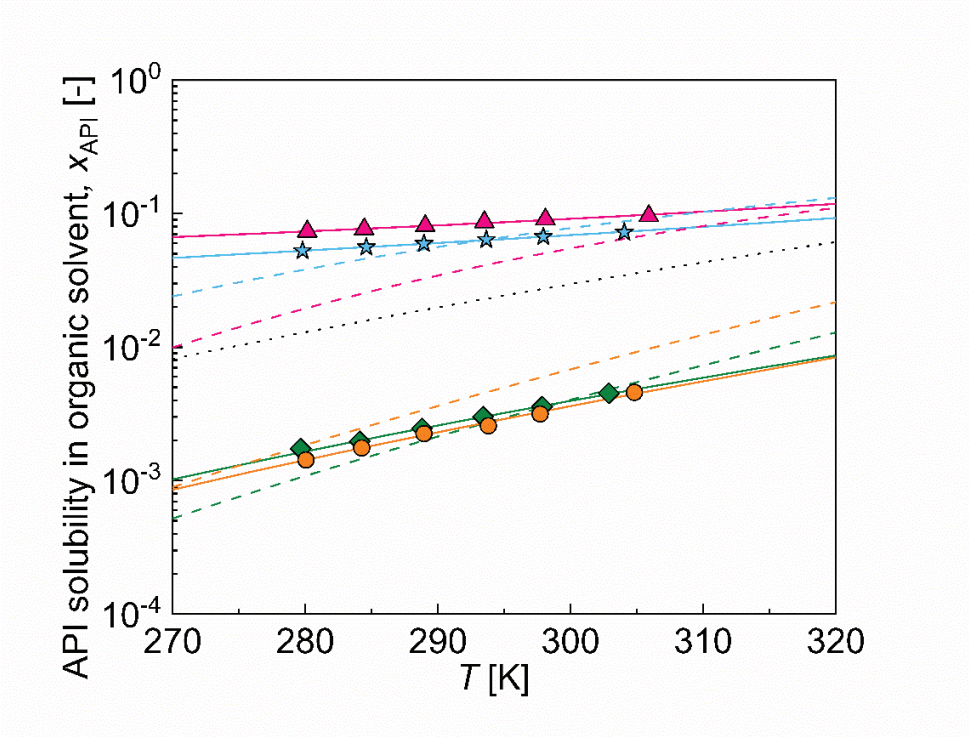

Figure 4-3. The measured solubility values of salsalate in acetone (▲:this study), ethyl acetate (★:this study), o-xylene (◆:this study) , and toluene (●:this study). The dashed lines denote the produced results by PC-SAFT when the pure-component parameters of salsalate are used as adjustable parameters in the case k_{ij} =0, where solid lines denote the produced results in the case k_{ij} is used as an additional adjustable parameter. The dotted line denotes the results for the ideal solubility case (γ_{API} =1)

Table 4-6. ARDs between the experimental and calculated solubility values by PC-SAFT for salsalate in organic solvents, and kij (binary interaction parameter) in Eq. (3-5).

APIs	Solvents	Experimental data sources of solubility values	ARD (k_{ij}=0) [%][a]	$k_{ij,\text{slope}} \times 10^4$ [K^{-1}][b]	$k_{ij,\text{intercept}}$ [-][b]	ARD (with k_{ij}) [%][c]
Salsalate	Toluene	This work	57.7	4.1	-0.11	2.5
	Ethyl acetate	This work	14.23	7.9	-0.23	0.33
	Acetone	This work	54.6	9.3	-0.3	1.01
	o-Xylene	This work	17.4	4.2	-0.12	1.72
	Overall		37.54			1.4

a: Average relative deviation for each solvent calculated using Eq. (3-10) by fitting the results produced by PC-SAFT with k_{ij} in Eq. (3-5) set to zero.
b: Parameters in Eq. (4-1).

c: ARD of the additional fitting using k_{ij} in Eq. (3-5).

Table 4-7. Molar mass and PC-SAFT pure-component parameters for the used APIs

APIs	M_i [g/mol]	m_i [-][a]	σ_i[Å] [a]	u_i/k_B [K] [a]	ARD [%][b]
Ibuprofen	206.29	5.6336	3.8384	221.37	11.5
Ketoprofen	254.28	2.3977	5.3035	281.04	14.7
Salsalate	258.23	1.9158	6.1038	288.14	37.5

a: Determined in this study by fitting to the solubility values of the APIs in organic solvents.
b: Average relative deviation calculated using Eq. (3-10) by fitting the results produced by PC-SAFT to the experimental data for each API using three PC-SAFT pure-component parameters with k_{ij} in Eq. (3-5) set to zero.

4.1.3. Validation of the determined pure component parameters of PC-SAFT for the investigated APIs

The relationship between the determined PC-SAFT pure component parameters and the selected solvents' physical properties was investigated to confirm the fitting results. According to published studies, the value of the $m_i\sigma_i^3$ expression (where m_i is the segment number, and σ_i is the segment diameter) of an organic solvent *i* varied linearly with the molar mass (M_i) of the solvent, and thus the expression was plotted vs the molar mass of salsalate, several organic solvents in addition to the two APIs studied before (ibuprofen and ketoprofen) in **Figure 4-4.** the obtained results verified that the APIs studied in this work follow the established trend of the relationship between the PC-SAFT pure component

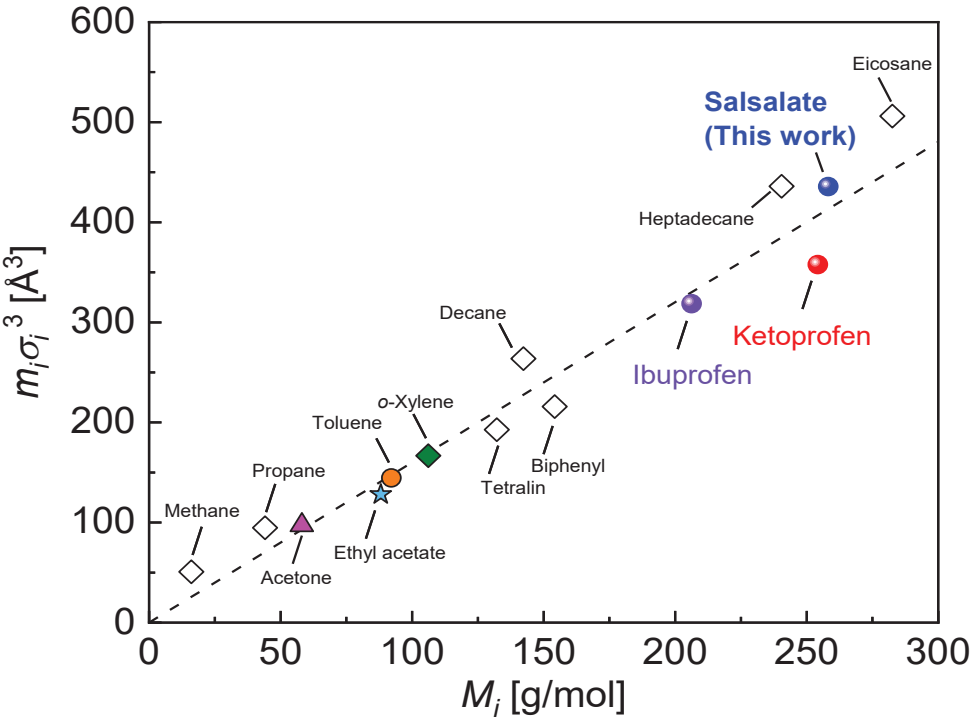

Figure 4-4. Validation of the PC-SAFT parameters of the used APIs in this work

4.1.4. Additional fitting using k_{ij}

There is a deviation between the experimental and the estimation results for the solubility of each of the investigated APIs in organic solvents, this deviation is demonstrated in the tables and figures of section 4.1.2. The reason for this deviation could be attributed to the interaction between the APIs and the used organic solvents that was not accounted for when *kij* is set to zero. Therefore, a new set of calculations was performed where the effect of *kij* was taken into consideration by using it as an additional fitting parameter. The results for these calculations are detailed in **Table S-1**, **Table S-2**, and **Table S-3** for ibuprofen, ketoprofen, and salsalate respectively, and are illustrated by the solid lines in **Figure 4-5**, **Figure 4-6**, and **Figure 4-7**.

As expected, those new results show better accuracy than the estimation results. The k_{ij} values were calculated according to the Eq. (4-1) with the values summarized in **Table S-1**, **Table S-2**, and **Table S-3** in Appendix I for the three APIs. The results for both estimation and correlation cases show that PC-SAFT can describe the solubility trends of the studied API-organic solvents systems.

$$k_{ij} = k_{ij,\text{slope}} T + k_{ij,\text{intercept}} \quad (4\text{-}1)$$

4.2. Estimating the solubility of APIs in $scCO_2$ using PC-SAFT

4.2.1. Estimating Isothermal solubility of drugs in $scCO_2$

The determined PC-SAFT pure component parameters for the investigated drugs in the previous section were used to estimate their solubility values in $scCO_2$ at the studied range of temperatures and pressures. The dashed lines in **Figure 4-5, Figure 4-6**, and **Figure 4-7**, show the estimation results for ibuprofen, ketoprofen and salsalate in $scCO_2$ obtained by PC-SAFT when k_{ij} was set to zero, with the corresponding ARD values listed in **Table 4-8**, **Table 4-9** and **Table 4-10** respectively. The solubility values were plotted vs pressure and vs the density of the supercritical fluid.

The published studies for the solubility of solid APIs in $scCO_2$ found that in general, the solubility of the solid solute increase with the increase in pressure[94]. This is because of the increase in the supercritical fluid density and consequently its dissolving power as the intermolecular distances decrease. This in turn promote interactions between the supercritical fluid and the solid solute molecules leading to an increase in solubility[144].

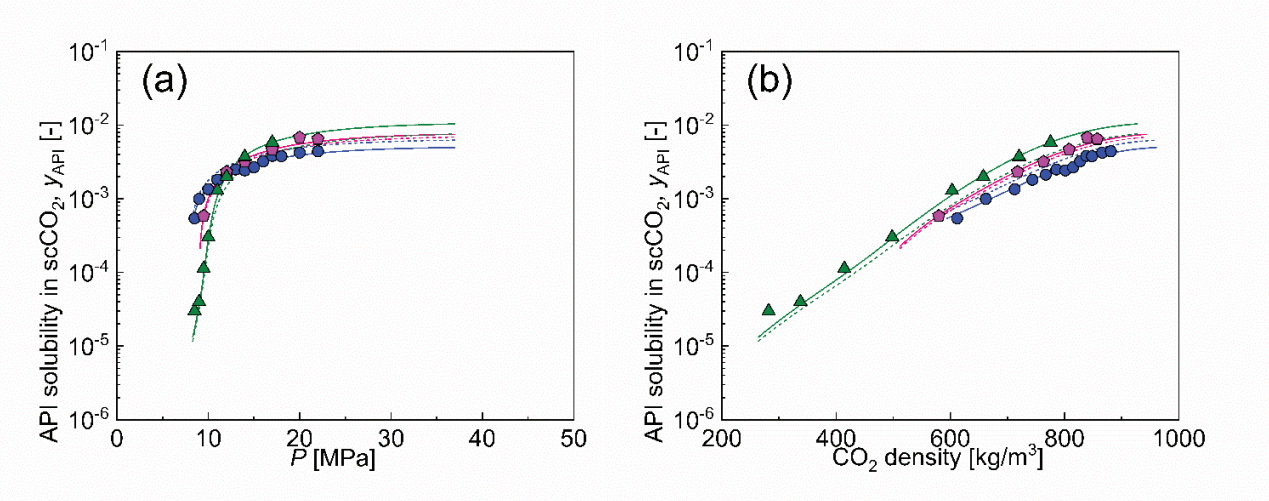

Figure 4-5. Isothermal solubility of ibuprofen in $scCO_2$ plotted vs (a) pressure and (b) CO_2 density. Symbols: literature experimental data at 318 K (▲[102]), 313 K (⬟,[102]), and 308 K (●,[102]); the dashed lines illustrate the estimated results using PC-SAFT in the case k_{ij} =0, and the solid lines show the obtained results PC-SAFT when k_{ij} of Eq. (3-5) is used as a fitting parameter.

Table 4-8. The estimated and correlated solubilities for ibuprofen in $scCO_2$ by PC-SAFT and the obtained k_{ij} at 8.5-30 MPa

API	T [K]	Reference	$ARD_{estimation}$ [%][a]	$ARD_{correlation}$ [%][b]	k_{ij} [-]
Ibuprofen	318	[102]	30.7	11.4	−0.0091
	313	[102]	10.5	6.6	−0.0023
	308	[102]	48.9	20.4	0.0057
	Overall		35.9	14.7	

a: Deviation defined with Eq. (3-10) at k_{ij}=0 in Eq. (3-5)
b: Deviation defined with Eq. (3-10) at k_{ij}= as an additional adjustable parameter

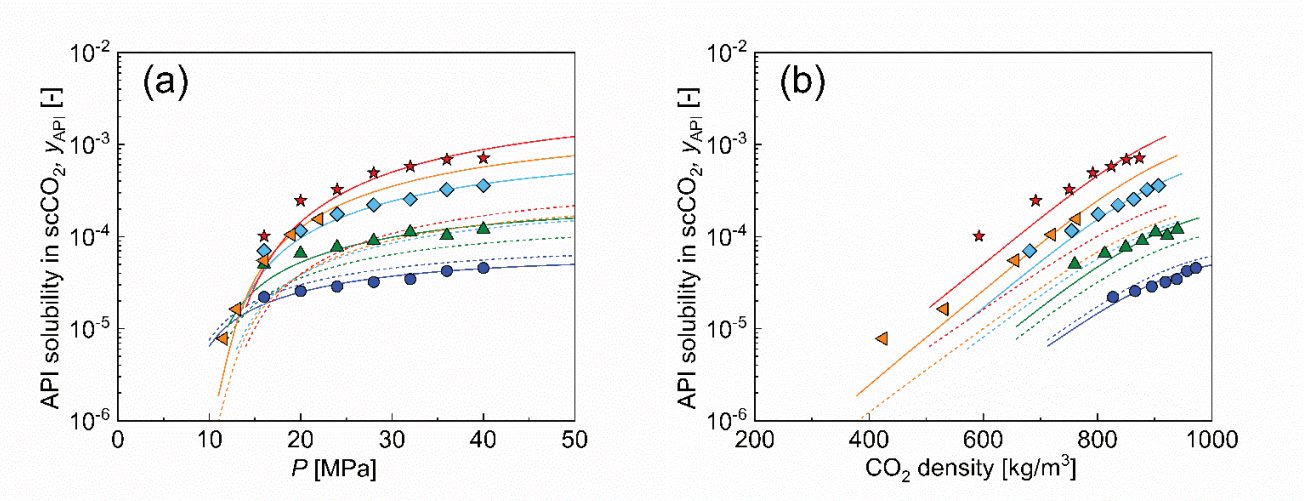

Figure 4-6. Isothermal solubility of ketoprofen in $scCO_2$ plotted vs (a) pressure and (b) CO_2 density. Symbols: literature experimental data at 338 K(★,[67]) , 331 K (▶,[64]), 328 K (◆,[67]), 318 K (▲,[67]), and 308 K (●,[67]); the dashed lines illustrate the estimated results using PC-SAFT in the case k_{ij} =0, and the solid lines show the obtained results PC-SAFT when k_{ij} of Eq. (3-5) is used as a fitting parameter.

Table 4-9.The estimated and correlated solubilities for Ketoprofen in $scCO_2$ by PC-SAFT and the obtained k_{ij} at 9-40 MPa

APIs	T [K]	Reference	$ARD_{estimation}$ [%][a]	$ARD_{correlation}$ [%][b]	k_{ij} [-]
Ketoprofen	338	[67]	80.5	22.2	−0.0483
	331	[64]	70.6	21.0	−0.0398
	328	[67]	66.9	11.4	−0.0302
	318	[67]	38.2	13.8	−0.0114
	308	[67]	23.6	7.0	0.0049
	Overall		55.1	14.7	

a: Deviation defined with Eq. (3-10) at k_{ij}=0 in Eq. (3-5)
b: Deviation defined with Eq. (3-10) at k_{ij}= as an additional adjustable parameter

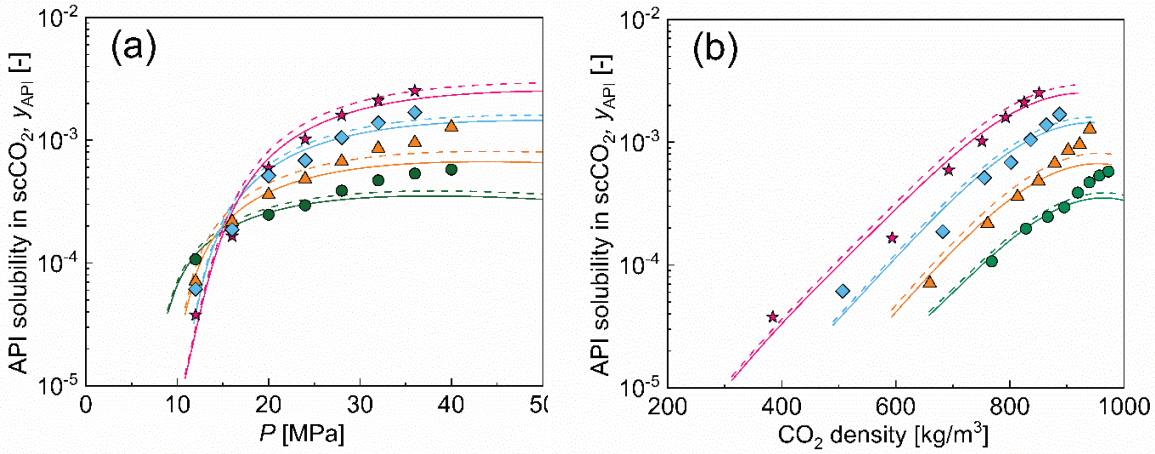

Figure 4-7. The Isothermal solubility of salsalate in $scCO_2$ as a function of (a) pressure and (b) CO_2 density. Symbols: literature experimental data at 308K(●,[103]), 318K(▲,[103]), 328K(◆,[103]),338K(★,[103]); the dashed lines illustrate the estimated results using PC-SAFT in the case k_{ij} =0, and the solid lines show the obtained results PC-SAFT when k_{ij} of Eq. (3-5) is used as a fitting parameter.

Table 4-10. The results of the estimated and correlated isothermal solubility of salsalate in $scCO_2$ using PC-SAFT EoS at pressures from 12-40 MPa.

API	T [K]	Reference	$ARD_{estimation}$ [%][a]	$ARD_{correlation}$ [%][b]	k_{ij} [-]
Salsalate	338	[103]	28.2	23.2	0.0047
	328	[103]	26.7	24.5	0.0027
	318	[103]	22.1	19.6	0.0047
	308	[103]	17.5	16.5	0.0021
	Overall		23.7	21.0	0.00354

a: Deviation defined with Eq. (3-10) at k_{ij}=0 in Eq.(3-5)
b: Deviation defined with Eq. (3-10) at k_{ij}= as an additional adjustable parameter

The same studies [94], [144] found two different patterns for the effect of temperature on the solubility of solid solutes in $scCO_2$ depending on the system pressure, where the solubility is directly proportional to the temperature beyond a pressure range called "The crossover region" and is inversely proportional below it. This could be explained by dual effect temperature have on the solid solute- supercritical fluid system, where its increase causes a decrease in the supercritical fluid density which leads to a decrease in solubility, but it also causes an increase in the vapor pressure of the solute reinforcing solubility. Below the cross over region, the density impact dominates and hence solubility decreases with increase in temperature, but the effect of vapor pressure is superior at higher pressures beyond this region causing the increase of solubility with the increase in temperature[145].

4.2.2. Additional fitting of the isothermal solubility in $scCO_2$ using k_{ij}

A deviation between the experimental and estimation values of the solubility of the investigated drugs can be observed in the previous figures. As in the organic solvents' fits, this also may be tracked to the effect of not considering the binary interaction parameter kij and thus the effect of intermolecular interactions between the API and the supercritical fluid. Therefore, additional fits using the value of kij as an adjustable parameter were performed. They are represented by the solid lines in **Figures 4-5, 4-6**, and **4-7** for each of the investigated drugs. The detailed results of the fits are listed in **Tables S-4**, **S-5** and **S-6** in Appendix I.

The results shown in **Tables S-4**, **S-5**, and **S-6** and Figures **4-5**, **4-6**, and **4-7** show that the correlated results using k_{ij} as an adjustable parameter are more accurate than the estimation results for ibuprofen and ketoprofen. In the salsalate case, only a slight improvement in the accuracy of the produced fits is possible when k_{ij} is used as an additional fitting parameter, also, the k_{ij} values in Table 4-13 remained nearly constant at a value close to zero over the investigated temperature range. That can be explained by the interaction between the supercritical fluid and salsalate for the investigated range of temperature, which can be satisfactorily accounted for using the Lorentz-Bertholet combining rules as in Eqs. (3-4) and (3-5), when k_{ij} is set as zero.

In **Figure 4-8**, the k_{ij} values, acquired by fitting the experimental solubility values of ibuprofen and ketoprofen in $scCO_2$ by PC-SAFT, are plotted as a function of temperature. For the range of temperatures studied, k_{ij} decreased linearly with the increase in temperature denoting that the interaction between the API and $scCO_2$ increased with temperature.

The k_{ij} values were fit using the least squares method and are formulated in Eqs. (4-2), and (4-3) for ibuprofen and ketoprofen respectively. These generalized values can ease the interpolation and extrapolation of the solubility at other temperatures, it is worth noting the produced relationship cannot be extended to other APIs

$$k_{ij} = -1.473 \times 10^{-3} T + 0.4595 \quad (4\text{-}2)$$

$$k_{ij} = -1.835 \times 10^{-3} T + 0.571 \quad (4\text{-}3)$$

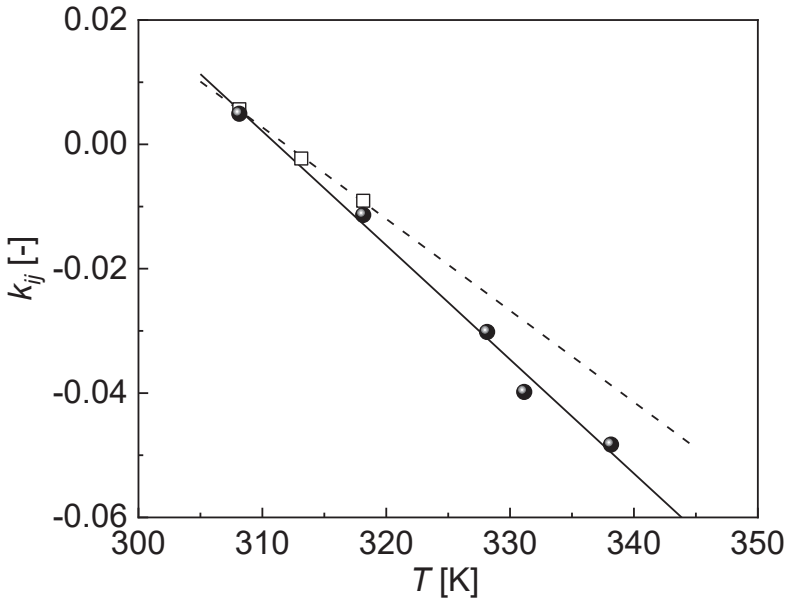

Figure 4-8 k_{ij} as a function of temperature (**Tables 4-8 and 4-9)**, obtained by fits to the API solubility in $scCO_2$ for ibuprofen (□, dashed line: Eq. (4-2)) and ketoprofen (●, solid line: Eq. (4-3) using PC-SAFT.

4.2.3. Calculating the isobaric solubility of APIs in $scCO_2$

Figures 4-9, **4-10**, and **4-11** demonstrates the results of the isobaric solubility of the investigated drugs in $scCO_2$ at temperatures from 308-338 K using PC-SAFT and the generalized k_{ij} for ibuprofen and Ketoprofen, and the average value of k_{ij} for Salsalate at the investigated temperatures (=0.00354). The dashed lines accounts for the estimated solubility values when k_{ij} was set to zero, while the solid lines account for the correlated solubility values when k_{ij} was used as a fitting parameter.

The solubilities acquired by the interpolation and extrapolation of literature values by the spline method are represented by the symbols in **Figures 4-9**, **4-10**, and **4-11** the corresponding values are listed in **Tables 4-11**, **4-12**, and **4-13**. Looking at those figures and

tables, we can deduce that the PC-SAFT equation of state coupled with the generalized k_{ij} can be used to describe the isobaric solubility of ibuprofen, ketoprofen and salsalate in $scCO_2$ at the studied range in this investigation.

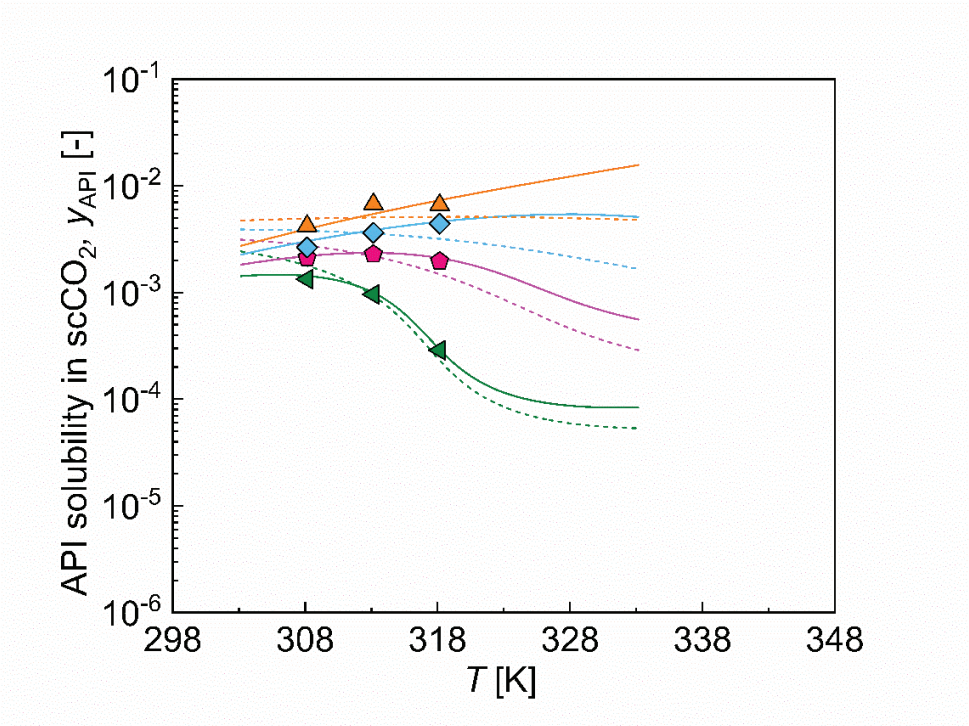

Figure 4-9. Isobaric solubility values of ibuprofen in $scCO_2$. Symbols represent experimental solubility data at 20.0 MPa (▲), 15.0 MPa (◆), 12.0 MPa (⬟), and 10.0 MPa (◀). dashed lines: estimations with PC-SAFT at k_{ij} = 0; solid lines: calculation with PC-SAFT using the generalized k_{ij} in Eq. (4-2)

Table 4-11. Results for the isobaric solubility of ibuprofen in $scCO_2$

APIs	P [MPa]	$ARD_{estimation}$ [%][a]	$ARD_{calculation}$ [%][b]
Ibuprofen	20.0	21.6	12.0
	15.0	24.3	8.1
	12.0	19.8	4.7
	10.0	18.9	4.4
	Overall	24.1	7.3

a: The estimated ARD for according to Eq. (3-10) at k_{ij} =0 in Eq (3-5).
b: The correlated ARD according to Eq. (3-10), using the average value of k_{ij}

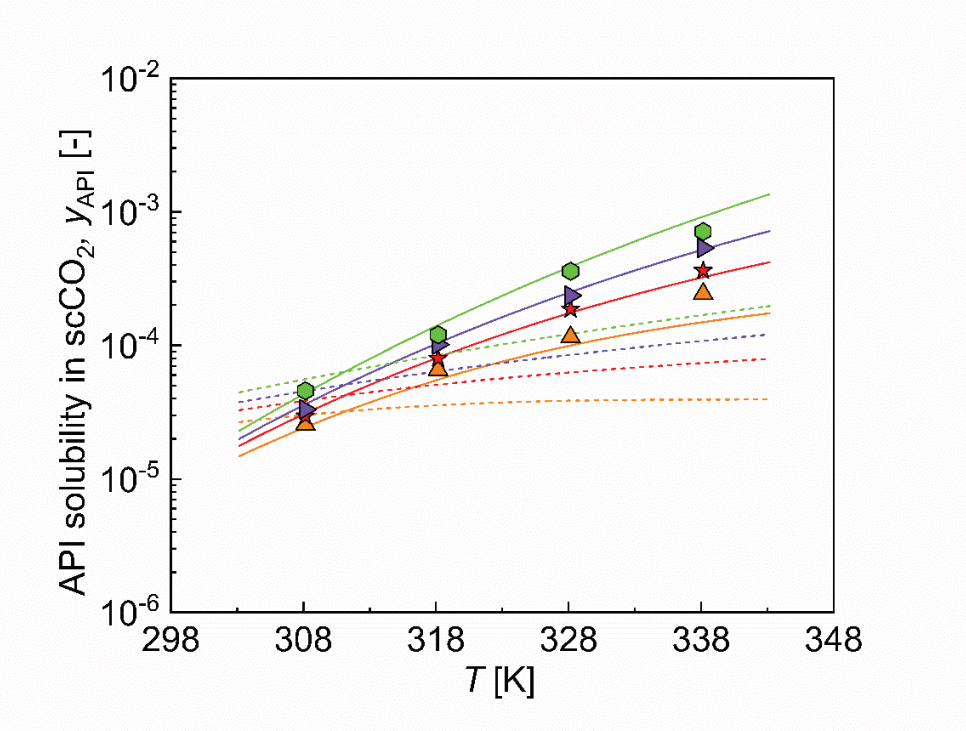

Figure 4-10. Isobaric solubility for Ketoprofen in $scCO_2$ at 40.0 MPa (⬣), 30.0 MPa ▶), 25.0 MPa (★), and 20.0 MPa (▲); dashed lines: estimations with PC-SAFT at k_{ij} = 0; solid lines: calculation with PC-SAFT using the generalized k_{ij} in Eq. (4-3).

Table 4-12. The isobaric solubility results for ketoprofen in $scCO_2$

APIs	P [MPa]	$ARD_{prediction}$ [%][a]	$ARD_{calculation}$ [%][b]
Ketoprofen	40.0	48.6	14.8
	30.0	54.5	5.4
	25.0	53.2	5.8
	20.0	53.5	18.0
	Overall	52.5	11.0

a: The estimated ARD for according to Eq. (3-10) at k_{ij} =0 in Eq (3-5).
b: The correlated ARD according to Eq. (3-10), using the average value of k_{ij}

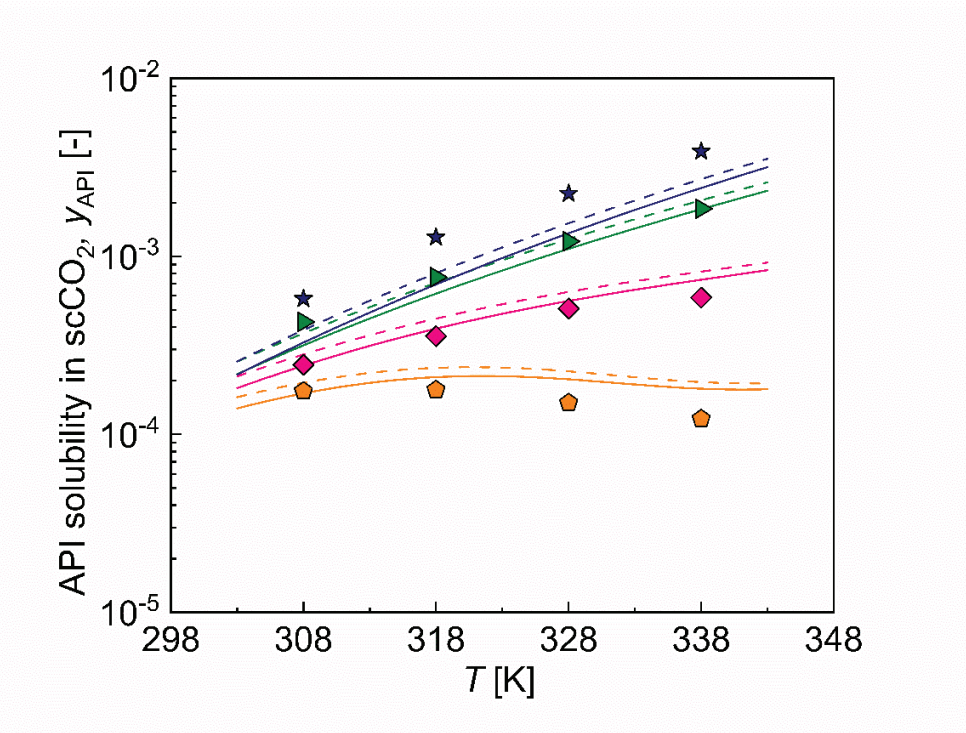

Figure 4-11. Isobaric solubility values of Salsalate in $scCO_2$. Symbols: experimental solubility data acquired through the extrapolation and interpolation of the literature values at 40.0 MPa (★), 30.0 MPa (▶), 20.0 MPa (◆), and 15.0 MPa (⬟); dashed lines illustrates for the estimations conducted with PC-SAFT at k_{ij} = 0; solid lines represent the correlation calculations with PC-SAFT using the average value of k_{ij} in Eq.(3-5)

Table 4-13. Results of the isobaric solubility calculations by PC-SAFT for salsalate in $scCO_2$

APIs	P [MPa]	$ARD_{estimation}$ [%][a]	$ARD_{calculation}$ [%][b]
Salsalate	40.0	33	41.6
	30.0	8.8	13.7
	20.0	26	11.9
	15.0	38.8	26
	Overall	26.65	23.3

a: The estimated ARD for according to Eq. (3-10) at k_{ij} =0 in Eq (3-5).
b: The correlated ARD according to Eq. (3-10), using the average value of k_{ij}

Figures 4-9, **4-10**, and **4-11** and **Tables 4-11**, **4-12**, and **4-13** show that PC-SAFT was successful in describing the investigated system isobaric solubility.

Chapter 5 : Summary of the study and recommendations for future work

Supercritical fluids technology is a solution to some of the challenges that face the pharmaceutical industry such as the low bioavailability of new candidate drugs, the development of green processes with minimal environmental impact, and the processing of thermally labile drugs, it can also help to obtain a final product that is free of solvents. That is all possible thanks to the lucrative properties of supercritical fluids which combines the solvency power of liquids with the transport properties of gases in addition to mild critical temperature and pressure, and the ease of removal and recycling. Therefore, supercritical fluid technology has been used in multiple processes in the pharmaceutical industry.

Knowledge of solubility in supercritical fluids is central to any process that employs them, including the process of production of delivery systems for controlled release. However, the high cost and the complexity of instruments needed to conduct the necessary experimental work, the vastness of APIs with each of them having different structures and functional groups, and the unsuitability of the popular modeling methods for the estimation of solubility proved to be challenges that need to be tackled.

This study suggests a novel approach using PC-SAFT EoS, which has better predictive capabilities than the commonly used cubic equations of state, to conduct the solubility calculations and utilizes the solubility data of the APIs in organic solvents to determine the necessary pure component parameters that PC-SAFT needs. Three model drugs were chosen

and their literature data along with new experimental data was investigated and measured. The solubility of ketoprofen and salsalate in several organic solvents was measured in this work and the literature data of ibuprofen was employed as well. PC-SAFT calculations were carried out to fit the pure components parameters of the drugs which are necessary to estimate and correlate the APIs solubility in supercritical carbon dioxide where the binary interaction coefficient k_{ij} was set as zero in the estimation calculations and used as an adjustable parameter in the correlation calculations. Generalized relations for k_{ij} was formulated and then used to calculate isobaric solubility values. PC-SAFT was found to reproduce the experimental solubility values satisfactorily for the studied drugs at the investigated range of pressures and temperatures.

A future area of research in this work could be the investigation of the solubility of more drugs to consolidate and validate the proposed approach. Other variations of SAFT that consider the effect of association by hydrogen bonds, and the quadrupolar interactions may provide a clearer understanding of the solubility process. Finally, extending the work into the second stage of the supercritical deposition process (adsorption) is a possible research direction to obtain a model that could describe the whole process.

References

[1] M. Pantić, Ž. Knez, and Z. Novak, “Supercritical impregnation as a feasible technique for entrapment of fat-soluble vitamins into alginate aerogels,” *J. Non Cryst. Solids*, vol. 432, pp. 519–526, 2016, doi: 10.1016/j.jnoncrysol.2015.11.011.

[2] G. Tkalec, M. Pantić, Z. Novak, and Ž. Knez, “Supercritical impregnation of drugs and supercritical fluid deposition of metals into aerogels,” *J. Mater. Sci.*, vol. 50, no. 1, pp. 1–12, 2015, doi: 10.1007/s10853-014-8626-0.

[3] A. Shivakalyani and S. Ramakrishna, “Controlled Drug Delivery Systems : Current Status and Future Directions,” *Molecules*, vol. 26, pp. 5905–5949, 2021, doi: https://doi.org/10.3390/molecules26195905.

[4] D. Bolten, R. Lietzow, and M. Türk, “Solubility of Ibuprofen, Phytosterol, Salicylic Acid, and Naproxen in Aqueous Solutions,” *Chem. Eng. Technol.*, vol. 36, no. 3, pp. 426–434, 2013, doi: 10.1002/ceat.201200510.

[5] L. Padrela, M. A. Rodrigues, A. Duarte, A. M. A. Dias, M. E. M. Braga, and H. C. de Sousa, “Supercritical carbon dioxide-based technologies for the production of drug nanoparticles/nanocrystals – A comprehensive review,” *Adv. Drug Deliv. Rev.*, vol. 131, pp. 22–78, 2018, doi: 10.1016/j.addr.2018.07.010.

[6] B. William, P. Noémie, E. Brigitte, and P. Géraldine, “Supercritical fluid methods: An alternative to conventional methods to prepare liposomes,” *J. Chem. Eng.*, vol. 383, 2020, doi: 10.1016/j.cej.2019.123106.

[7] Y. A. Hussain and C. S. Grant, “Ibuprofen impregnation into submicron polymeric

films in supercritical carbon dioxide," *J. Supercrit. Fluids,* , vol. 71, pp. 127–135, 2012, doi: 10.1016/j.supflu.2012.07.014.

[8] E. M. Martín Del Valle, M. A. Galán, and R. G. Carbonell, "Drug Delivery Technologies: The Way Forward in the New Decade," *Ind. Eng. Chem. Res.*, vol. 48, pp. 2475–2486, 2009, doi: 10.1021/ie800886m.

[9] M. Champeau, J. M. Thomassin, T. Tassaing, and C. Jérôme, "Drug loading of polymer implants by supercritical CO2 assisted impregnation: A review," *J. Control. Release.*, vol. 209, pp. 248–259, 2015, doi: 10.1016/j.jconrel.2015.05.002.

[10] Y. Yokozaki and Y. Shimoyama, "Loading of vitamin E into silicone hydrogel by supercritical carbon dioxide impregnation toward controlled release of timolol maleate," *J. Supercrit. Fluids*, vol. 131, pp. 11–18, 2018, doi: 10.1016/j.supflu.2017.08.010.

[11] K. J. Rambhia and P. X. Ma, "Controlled drug release for tissue engineering," *J. Control. Release*, vol. 219, pp. 119–128, 2015, doi: 10.1016/j.jconrel.2015.08.049.

[12] E. Sayed, R. Haj-Ahmad, K. Ruparelia, M. S. Arshad, M. W. Chang, and Z. Ahmad, "Porous Inorganic Drug Delivery Systems—a Review," *AAPS Pharm. Sci. Tech.*, vol. 18, no. 5, pp. 1507–1525, 2017, doi: 10.1208/s12249-017-0740-2.

[13] N. Esfandiari, "Production of micro and nano particles of pharmaceutical by supercritical carbon dioxide," *J. Supercrit. Fluids*, vol. 100, pp. 129–141, 2015, doi: 10.1016/j.supflu.2014.12.028.

[14] V. Cauda and G. Canavese, "Mesoporous materials for drug delivery and theranostics," *Pharmaceutics*, vol. 12, no. 11, pp. 1–3, 2020, doi: 10.3390/pharmaceutics12111108.

[15] F. Ruether and G. Sawdowski, “Modeling the Solubility of Pharmaceuticals in Pure Solvents and Solvent Mixtures for Drug Process Design,” *J. Pharm. Sci.*, vol. 101, no. 7, pp. 2271–2280, 2012, doi: 10.1002/jps.

[16] S. W. Song, K. Hidajat, and S. Kawi, “Functionalized SBA-15 materials as carriers for controlled drug delivery: Influence of surface properties on matrix-drug interactions,” *Langmuir*, vol. 21, no. 21, pp. 9568–9575, 2005, doi: 10.1021/la051167e.

[17] L. Tarja, A. S. Helder, and E. Makila, “Molecular Nanomedicine Towards Cancer :,” *J. Pharm. Sci.*, vol. 100, no. 7, pp. 3294-3306], 2011, doi: 10.1002/jps.

[18] S. Hong *et al.*, “High drug load, stable, manufacturable and bioavailable fenofibrate formulations in mesoporous silica: A comparison of spray drying versus solvent impregnation methods,” *Drug Deliv.*, vol. 23, no. 1, pp. 316–327, 2016, doi: 10.3109/10717544.2014.913323.

[19] Knez, E. Markočič, M. Leitgeb, M. Primožič, M. Knez Hrnčič, and M. Škerget, “Industrial applications of supercritical fluids: A review,” *Energy*, vol. 77, pp. 235–243, 2014, doi: 10.1016/j.energy.2014.07.044.

[20] S. D. Manjare and K. Dhingra, “Supercritical fluids in separation and purification: A review,” *Mater. Sci. Energy Technol.*, vol. 2, no. 3, pp. 463–484, 2019, doi: 10.1016/j.mset.2019.04.005.

[21] M. Banchero and L. Manna, “Solubility of fenamate drugs in supercritical carbon dioxide by using a semi-flow apparatus with a continuous solvent-washing step in the depressurization line,” *J. Supercrit. Fluids*, vol. 107, pp. 400–407, 2016, doi: 10.1016/j.supflu.2015.10.008.

[22] T. T. Ngo *et al.*, “Drug impregnation for laser sintered poly(methyl methacrylate) biocomposites using supercritical carbon dioxide,” *J. Supercrit. Fluids*, vol. 136, pp. 29–36, 2018, doi: 10.1016/j.supflu.2018.01.030.

[23] H. Bagheri, G. Ali Mansoori, and H. Hashemipour, “A novel approach to predict drugs solubility in supercritical solvents for RESS process using various cubic EoS-mixing rule,” *J. Mol. Liq.*, vol. 261, pp. 174–188, 2018, doi: 10.1016/j.molliq.2018.03.081.

[24] P. Franco and I. de Marco, “Supercritical CO2 adsorption of non-steroidal anti-inflammatory drugs into biopolymer aerogels,” *J. CO2 Util.*, vol. 36, pp. 40–53, 2020, doi: 10.1016/j.jcou.2019.11.001.

[25] M. Khamda, M. H. Hosseini, and M. Rezaee, “Measurement and correlation solubility of cefixime trihydrate and oxymetholone in supercritical carbon dioxide (CO2),” *J. Supercrit. Fluids*, vol. 73, pp. 130–137, 2013, doi: 10.1016/j.supflu.2012.09.006.

[26] A. Tabernero, E. M. Martín del Valle, and M. A. Galán, “Supercritical fluids for pharmaceutical particle engineering: Methods, basic fundamentals and modelling,” *Chem. Eng. Process.*, vol. 60. pp. 9–25, 2012. doi: 10.1016/j.cep.2012.06.004.

[27] G. Sodeifian and S. A. Sajadian, “Solubility measurement and preparation of nanoparticles of an anticancer drug (Letrozole) using rapid expansion of supercritical solutions with solid cosolvent (RESS-SC),” *J. Supercrit. Fluids*, vol. 133, 2017, pp. 239–252, 2018, doi: 10.1016/j.supflu.2017.10.015.

[28] G. Sodeifian, S. M. Hazaveie, S. A. Sajadian, and F. Razmimanesh, “Experimental investigation and modeling of the solubility of oxcarbazepine (an anticonvulsant agent)in supercritical carbon dioxide,” *Fluid Phase Equilib.*, vol. 493, pp. 160–173,

2019, doi: 10.1016/j.fluid.2019.04.013.

[29] G. Sodeifian, F. Razmimanesh, S. A. Sajadian, and S. M. Hazaveie, “Experimental data and thermodynamic modeling of solubility of Sorafenib tosylate, as an anti-cancer drug, in supercritical carbon dioxide: Evaluation of Wong-Sandler mixing rule,” *J. Chem. Thermodyn.*, vol. 142, p. 105998, 2020, doi: 10.1016/j.jct.2019.105998.

[30] S. A. B. Vieira De Melo, R. L. F. Vieira De Melo, G. M. N. Costa, and T. L. M. Alves, “Solubility of l-Dopa in supercritical carbon dioxide: Prediction using a cubic equation of state,” *J. Supercrit. Fluids*, vol. 34, no. 2 SPEC. ISS., pp. 231–236, 2005, doi: 10.1016/j.supflu.2004.11.019.

[31] G. N. Escobedo-Alvarado, S. I. Sandler, and A. M. Scurto, “Modeling of solid-supercritical fluid phase equilibria with a cubic equation of state - Gex model,” *J. Supercrit. Fluids*, vol. 21, no. 2, pp. 123–134, 2001, doi: 10.1016/S0896-8446(01)00092-4.

[32] J. Gross and G. Sadowski, “Application of the Perturbed-Chain SAFT equation of state to associating systems,” *Fluid Phase Equilib.*, vol. 217, no. 41, pp. 5510–5515, 2002, doi: 10.1016/j.fluid.2002.12.002.

[33] J. Gross and G. Sadowski, “Perturbed-Chain SAFT: An Equation of State Based on a Perturbation Theory for Chain Molecules,” *Ind. Eng. Chem. Res.*, vol. 40, pp. 1244–1260, 2001, doi: 10.1021/ie0003887.

[34] M. Kleiner and G. Sadowski, “Modeling of polar systems using PCP-SAFT: An approach to account for induced-association interactions,” *J. Phys. Chem. C*, vol. 111, no. 43, pp. 15544–15553, 2007, doi: 10.1021/jp072640v.

[35] C. H. Bang and B. S. Lee, “Modeling phase behavior of Poly(ε-caprolactone) solutions at high pressure,” *Fluid Phase Equilib.*, vol. 483, pp. 116–121, 2019, doi: 10.1016/j.fluid.2018.11.008.

[36] M. L. Corazza, W. A. Fouad, and W. G. Chapman, “Application of molecular modeling to the vapor-liquid equilibrium of alkyl esters (biodiesel) and alcohols systems,” *Fuel*, vol. 161, pp. 34–42, 2015, doi: 10.1016/j.fuel.2015.08.003.

[37] P. Navarro, A. M. Palma, J. García, F. Rodríguez, J. A. P. Coutinho, and P. J. Carvalho, “High pressure density of tricyanomethanide-based ionic liquids: Experimental and PC-SAFT modelling,” *Fluid Phase Equilib.*, vol. 520, pp. 4–11, 2020, doi: 10.1016/j.fluid.2020.112652.

[38] N. I. Diamantonis and I. G. Economou, “Evaluation of Statistical Associating Fluid Theory (SAFT) and Perturbed Chain-SAFT Equations of State for the Calculation of Thermodynamic Derivative Properties of Fluids Related to Carbon Capture and Sequestration,” *Energy Fuels.*, vol. 25, pp. 4–11 pp. 3334–3343, 2011, doi: 10.1021/ef200387p

[39] R. Paus, Y. Ji, L. Vahle, and G. Sadowski, “Predicting the Solubility Advantage of Amorphous Pharmaceuticals: A Novel Thermodynamic Approach,” *Mol. Pharm.*, vol. 12, no. 8, pp. 2823–2833, 2015, doi: 10.1021/mp500824d.

[40] T. Fujii, Y. Matsuo, and S. I. Kawasaki, “Rapid Continuous Supercritical CO2 Extraction and Separation of Organic Compounds from Liquid Solutions,” *Ind. Eng. Chem. Res.*, vol. 57, no. 16, pp. 5717–5721, 2018, doi: 10.1021/acs.iecr.8b00812.

[41] R. Kumar, A. K. Thakur, N. Banerjee, and P. Chaudhari, “Investigation on

crystallization phenomena with supercritical carbon dioxide (CO2) as the antisolvent," *Int. J. Chem. React.*, vol. 19, no. 8, pp. 861–871, 2021, doi: 10.1515/ijcre-2020-0189.

[42] G. Caputo, M. Scognamiglio, and I. de Marco, "Nimesulide adsorbed on silica aerogel using supercritical carbon dioxide," *Chem. Eng. Res. Des.*, vol. 90, no. 8, pp. 1082–1089, 2012, doi: 10.1016/j.cherd.2011.11.011.

[43] M. Türk, "Manufacture of submicron drug particles with enhanced dissolution behaviour by rapid expansion processes," *J. Supercrit. Fluids*, vol. 47, no. 3, pp. 537–545, 2009, doi: 10.1016/j.supflu.2008.09.008.

[44] Y. Sun, Y. Ueda, H. Suganaga, M. Haruki, S. Kihara, and S. Takishima, "Experimental and simulation study of the physical foaming process using high-pressure CO2," *J. Supercrit. Fluids*, vol. 107. pp. 733–745, 2016. doi: 10.1016/j.supflu.2015.08.001.

[45] G. Brunner, "Supercritical fluids: Technology and application to food processing," *J. Food Eng.*, vol. 67, no. 1–2, pp. 21–33, 2005, doi: 10.1016/j.jfoodeng.2004.05.060.

[46] D. E. Knox, "Solubilities in supercritical fluids," *Pure Appl. Chem.*, vol. 77, no. 3, pp. 513–530, 2005, doi: 10.1351/pac200577030513.

[47] H. B. Rad, J. K. Sabet, and F. Varaminian, "Study of solubility in supercritical fluids: Thermodynamic concepts and measurement methods - A review," *Braz. J. Chem. Eng.*, vol. 36, no. 4, pp. 1367–1392, 2019, doi: 10.1590/0104-6632.20190364s20170493.

[48] M. Shamsipur, M. R. Fat'hi B, Y. Yamini, and A. R. Ghiasvand, "Solubility determination of nitrophenol derivatives in supercritical carbon dioxide,", *J. Supercrit. Fluids,* vol. 23, pp.225-231, 2002. doi: 10.1016/S0896-8446(01)00143-7.

[49] Z. Huang, X. W. Yang, G. B. Sun, S. W. Song, and S. Kawi, "The solubilities of

xanthone and xanthene in supercritical carbon dioxide: Structure effect," *J. Supercrit. Fluids*, vol. 36, no. 2, pp. 91–97, 2005, doi: 10.1016/j.supflu.2005.04.002.

[50] H. Asiabi, Y. Yamini, M. Tayyebi, M. Moradi, A. Vatanara, and K. Keshmiri, "Measurement and correlation of the solubility of two steroid drugs in supercritical carbon dioxide using semi empirical models," *J. Supercrit. Fluids*, vol. 78, pp. 28–33, 2013, doi: 10.1016/j.supflu.2013.03.018.

[51] Z. Knez, M. Škerget, P. Sencar-Božic, and A. Rižner, "Solubility of Nifedipine and Nitrendipine in Supercritical CO2," *J. Chem. Eng. Data*, vol. 40, no. 1, pp. 216–220, 1995, doi: 10.1021/je00017a045.

[52] G. Sodeifian, F. Razmimanesh, and S. A. Sajadian, "Solubility measurement of a chemotherapeutic agent (Imatinib mesylate) in supercritical carbon dioxide: Assessment of new empirical model," *J. Supercrit. Fluids*, vol. 146, pp. 89–99, 2019, doi: 10.1016/j.supflu.2019.01.006.

[53] Y. M. Chen, P. C. Lin, M. Tang, and Y. P. Chen, "Solid solubility of antilipemic agents and micronization of gemfibrozil in supercritical carbon dioxide," *J. Supercrit. Fluids*, vol. 52, no. 2, pp. 175–182, 2010, doi: 10.1016/j.supflu.2009.12.012.

[54] M. Lashkarbolooki, A. Z. Hezave, Y. Rahnama, H. Rajaei, and F. Esmaeilzadeh, "Solubility of chlorpheniramine maleate in supercritical carbon dioxide," *J. Supercrit. Fluids*, vol. 84, pp. 29–35, 2013, doi: 10.1016/j.supflu.2013.09.007.

[55] M. Hojjati, Y. Yamini, M. Khajeh, and A. Vatanara, "Solubility of some statin drugs in supercritical carbon dioxide and representing the solute solubility data with several density-based correlations," *J. Supercrit. Fluids*, vol. 41, no. 2, pp. 187–194, 2007,

doi: 10.1016/j.supflu.2006.10.006.

[56] M. H. Hosseini, N. Alizadeh, and A. R. Khanchi, “Solubility analysis of clozapine and lamotrigine in supercritical carbon dioxide using static system,” *J. Supercrit. Fluids*, vol. 52, no. 1, pp. 30–35, 2010, doi: 10.1016/j.supflu.2009.11.006.

[57] K. Ongkasin, M. Sauceau, Y. Masmoudi, J. Fages, and E. Badens, “Solubility of cefuroxime axetil in supercritical CO2: Measurement and modeling,” *J. Supercrit. Fluids*, vol. 152, p. 104498, 2019, doi: 10.1016/j.supflu.2019.03.010.

[58] R. Heryanto, E. C. Abdullah, and M. Hasan, “Solubility of Isoniazid in Supercritical Carbon Dioxide Rudi,” *J. Chem. Eng. Data*, vol. 55, no. 9, pp. 3704–3707, 2010, doi: 10.1021/je100245n.

[59] A. Stassi, R. Bettini, A. Gazzaniga, F. Giordano, and A. Schiraldi, “Assessment of solubility of ketoprofen and vanillic acid in supercritical CO2 under dynamic conditions,” *J. Chem. Eng. Data*, vol. 45, no. 2, pp. 161–165, 2000, doi: 10.1021/je990114u.

[60] M. Ardjmand, M. Mirzajanzadeh, and F. Zabihi, “Measurement and correlation of solid drugs solubility in supercritical systems,” *Chin. J. Chem. Eng.*, vol. 22, no. 5, pp. 549–558, 2014, doi: 10.1016/S1004-9541(14)60073-2.

[61] K. Shi, L. Feng, L. He, and H. Li, “Solubility Determination and Correlation of Gatifloxacin, Enrofloxacin, and Ciprofloxacin in Supercritical CO2,” *J. Chem. Eng. Data*, vol. 62, no. 12, pp. 4235–4243, 2017, doi: 10.1021/acs.jced.7b00601.

[62] M. D. Gordillo, M. A. Blanco, A. Molero, and E. Martinez De La Ossa, “Solubility of the antibiotic Penicillin G in supercritical carbon dioxide,” *J. Supercrit. Fluids*, vol.

15, no. 3, pp. 183–190, 1999, doi: 10.1016/S0896-8446(99)00008-X.

[63] Z. Huang, W. D. Lu, S. Kawi, and Y. C. Chiew, “Solubility of aspirin in supercritical carbon dioxide with and without Acetone,” *J. Chem. Eng. Data*, vol. 49, no. 5, pp. 1323–1327, 2004, doi: 10.1021/je0499465.

[64] S. J. Macnaughton *et al.*, “Solubility of Anti-Inflammatory Drugs in Supercritical Carbon Dioxide,” *J. Chem. Eng. Data*, vol. 9568, no. 1991, pp. 1083–1086, 1996, doi: 10.1021/je960103q.

[65] H. Sovová, “Solubility of Ferulic Acid in Supercritical Carbon Dioxide with Ethanol as Cosolvent,” *J. Chem. Eng. Data*, vol. 46, pp. 1255–1257, 2001, doi: 10.1021/je0101146.

[66] D. Suleiman, L. Antonio Estévez, J. C. Pulido, J. E. García, and C. Mojica, “Solubility of anti-inflammatory, anti-cancer, and anti-HIV drugs in supercritical carbon dioxide,” *J. Chem. Eng. Data*, vol. 50, no. 4, pp. 1234–1241, 2005, doi: 10.1021/je049551l.

[67] M. A. Sabegh, H. Rajaei, F. Esmaeilzadeh, and M. Lashkarbolooki, “Solubility of ketoprofen in supercritical carbon dioxide,” *J. Supercrit. Fluids*, vol. 72, pp. 191–197, 2012, doi: 10.1016/j.supflu.2012.08.008.

[68] K. Ongkasin, Y. Masmoudi, T. Tassaing, G. Le-Bourdon, and E. Badens, “Supercritical loading of gatifloxacin into hydrophobic foldable intraocular lenses – Process control and optimization by following in situ CO2 sorption and polymer swelling,” *Int. J. Pharm.*, vol. 581, p. 119247, 2020, doi: 10.1016/j.ijpharm.2020.119247.

[69] P. Coimbra, D. Fernandes, P. Ferreira, M. H. Gil, and H. C. de Sousa, “Solubility of Irgacure® 2959 photoinitiator in supercritical carbon dioxide: Experimental

determination and correlation," *J. Supercrit. Fluids*, vol. 45, no. 3, pp. 272–281, 2008, doi: 10.1016/j.supflu.2008.01.014.

[70] R. Ratnawati, "Van Der Waals Mixing Rules for the Redlich-Kwong Equation of State. Application for Supercritical Solubility Modeling," *Reaktor*, vol. 10, no. 2, pp. 96–102, 2006, doi: 10.14710/reaktor.10.2.96-102.

[71] D. Peng, D. B. Robinson, D. Peng, and D. B. Robinson, "A New Two-Constant Equation of State A New Two-Constant Equation of State," *Ind. Eng. Chem. Fundam.*, vol. 15, no. 1, pp. 59–64, 1976.

[72] G. Soave, "Equilibrium constants from a modified Redlich-Kwong equation of state," *Chem. Eng. Sci.*, vol. 27, no. 6, pp. 1197–1203, 1972, doi: 10.1016/0009-2509(72)80096-4.

[73] G. M. Kontogeorgis and I. G. Economou, "Equations of state: From the ideas of van der Waals to association theories," *J. Supercrit. Fluids*, vol. 55, no. 2, pp. 421–437, 2010, doi: 10.1016/j.supflu.2010.10.023.

[74] W. G. Chapman, K. E. Gubbins, G. Jackson, and M. Radosz, "New reference equation of state for associating liquids," *Ind. Eng. Chem. Res.*, vol. 29, no. 8, pp. 1709–1721, 1990, doi: 10.1021/ie00104a021.

[75] A. Gil-Villegas, A. Galindo, P. J. Whitehead, S. J. Mills, G. Jackson, and A. N. Burgess, "Statistical associating fluid theory for chain molecules with attractive potentials of variable range," *Chem. Phys.*, vol. 106, no. 10, pp. 4168–4186, 1997, doi: 10.1063/1.473101.

[76] E. K. Karakatsani, T. Spyriouni, and I. G. Economou, "Extended statistical associating

fluid theory (SAFT) equations of state for dipolar fluids," *AIChE Journal*, vol. 51, no. 8, pp. 2328–2342, 2005, doi: 10.1002/aic.10473.

[77] G. Sodeifian, R. Detakhsheshpour, and S. A. Sajadian, "Experimental study and thermodynamic modeling of Esomeprazole (proton-pump inhibitor drug for stomach acid reduction) solubility in supercritical carbon dioxide," *J. Supercrit. Fluids*, vol. 154, p. 104606, 2019, doi: 10.1016/j.supflu.2019.104606.

[78] M. R. Housaindokht and M. R. Bozorgmehr, "Calculation of solubility of methimazole, phenazopyridine and propranolol in supercritical carbon dioxide," *J. Supercrit. Fluids*, vol. 43, no. 3, pp. 390–397, 2008, doi: 10.1016/j.supflu.2007.07.013.

[79] M. Hosseini Anvari and G. Pazuki, "A study on the predictive capability of the SAFT-VR equation of state for solubility of solids in supercritical CO2," *J. Supercrit. Fluids*, vol. 90, pp. 73–83, 2014, doi: 10.1016/j.supflu.2014.03.005.

[80] I. Kikic, N. de Zordi, M. Moneghini, and D. Solinas, "Solubility estimation of drugs in ternary systems of interest for the antisolvent precipitation processes," *J. Supercrit. Fluids*, vol. 55, no. 2, pp. 616–622, 2010, doi: 10.1016/j.supflu.2010.09.034.

[81] S. S. T. Ting, S. J. Macnaughton, D. L. Tomasko, and N. R. Foster, "Solubility of Naproxen in Supercritical Carbon Dioxide with and without Cosolvents," *Ind. Eng. Chem. Res.*, vol. 32, no. 7, pp. 1471–1481, 1993, doi: 10.1021/ie00019a022.

[82] G. Sodeifian, S. A. Sajadian, and F. Razmimanesh, "Solubility of an antiarrhythmic drug (amiodarone hydrochloride) in supercritical carbon dioxide: Experimental and modeling," *Fluid Phase Equilib.*, vol. 450, pp. 149–159, 2017, doi: 10.1016/j.fluid.2017.07.015.

[83] N. Lamba, R. C. Narayan, J. Modak, and G. Madras, “Solubilities of 10-undecenoic acid and geraniol in supercritical carbon dioxide,” *J. Supercrit. Fluids*, vol. 107, pp. 384–391, 2016, doi: 10.1016/j.supflu.2015.09.026.

[84] C. C. Tsai, H. M. Lin, and M. J. Lee, “Solubility of niflumic acid and celecoxib in supercritical carbon dioxide,” *J. Supercrit. Fluids*, 2014, doi: 10.1016/j.supflu.2014.07.026.

[85] J. Chrastil, “Solubility of Solids and Liquids in Supercritical Fluids,” *J. Phys. Chem.*, no. 86, pp. 3016–3021, 1982, doi: 10.1002/0470867833.ch13.

[86] D. L. Sparks, R. Hernandez, and L. A. Estévez, “Evaluation of density-based models for the solubility of solids in supercritical carbon dioxide and formulation of a new model,” *Chem. Eng. Sci.*, vol. 63, no. 17, pp. 4292–4301, 2008, doi: 10.1016/j.ces.2008.05.031.

[87] J. M. del Valle and J. M. Aguilera, “An Improved Equation for Predicting the Solubility of Vegetable Oils in Supercritical Co2,” *Ind. Eng. Chem. Res.*, vol. 27, no. 8, pp. 1551–1553, 1988, doi: 10.1021/ie00080a036.

[88] Y. Adachi and B. C. Y. Lu, “Supercritical fluid extraction with Carbon dioxide and Ethylene,” *Fluid Phase Equilib.*, vol. 1, no. 14, pp. 147–156, 1983, doi: 10.1016/0378-3812(83)80120-4.

[89] J. Méndez-Santiago and A. S. Teja, “The solubility of solids in supercritical fluids,” *Fluid Phase Equilib.*, vol. 158–160, pp. 501–510, 1999, doi: 10.1016/s0378-3812(99)00154-5.

[90] K. D. Bartle, A. A. Clifford, S. A. Jafar, and G. F. Shilstone, “Solubilities of Solids and

Liquids of Low Volatility in Supercritical Carbon Dioxide," *J. Phys. Chem. Ref. Data*, vol. 20, no. 4, pp. 713–756, 1991, doi: 10.1063/1.555893.

[91] A. Tabernero, E. M. Martín del Valle, and M. A. Galán, "Supercritical fluids for pharmaceutical particle engineering: Methods, basic fundamentals and modelling," *Chem. Eng. Process.*, vol. 60, pp. 9–25, 2012, doi: 10.1016/j.cep.2012.06.004.

[92] A. Tabernero, E. M. M. del Valle, and M. Á. Galán, "A comparison between semiempirical equations to predict the solubility of pharmaceutical compounds in supercritical carbon dioxide," *J. Supercrit. Fluids*, vol. 52, no. 2, pp. 161–174, 2010, doi: 10.1016/j.supflu.2010.01.009.

[93] S. A. Shojaee, H. Rajaei, A. Z. Hezave, M. Lashkarbolooki, and F. Esmaeilzadeh, "Experimental investigation and modeling of the solubility of carvedilol in supercritical carbon dioxide," *J. Supercrit. Fluids*, vol. 81, pp. 42–47, 2013, doi: 10.1016/j.supflu.2013.04.013.

[94] G. Sodeifian, S. A. Sajadian, and N. S. Ardestani, "Determination of solubility of Aprepitant (an antiemetic drug for chemotherapy) in supercritical carbon dioxide: Empirical and thermodynamic models," *J. Supercrit. Fluids*, vol. 128, pp. 102–111, 2017, doi: 10.1016/j.supflu.2017.05.019.

[95] M. H. Hosseini, N. Alizadeh, and A. R. Khanchi, "Effect of menthol as solid cosolvent on the solubility enhancement of clozapine and lamorigine in supercritical CO2," *J. Supercrit. Fluids*, vol. 55, no. 1, pp. 14–22, 2010, doi: 10.1016/j.supflu.2010.09.002.

[96] S. N. Reddy and G. Madras, "Solubilities of resorcinol and pyrocatechol and their mixture in supercritical carbon dioxide," *Thermochim. Acta*, vol. 521, no. 1–2, pp. 41–

48, 2011, doi: 10.1016/j.tca.2011.04.002.

[97] K. Matsuyama, K. Mishima, R. Ohdate, M. Chidori, and H. Yang, “3 , 3 ′ , 4 ′ , 5 , 7-Pentahydroxyflavone in Supercritical Carbon Dioxide,” *J. Chem. Eng. Data*, vol. 2, pp. 1040–1043, 2003, doi: 10.1021/je030129z.

[98] C. S. Su and Y. P. Chen, “Measurement and correlation for the solid solubility of non-steroidal anti-inflammatory drugs (NSAIDs) in supercritical carbon dioxide,” *J. Supercrit. Fluids*, vol. 43, no. 3, pp. 438–446, 2008, doi: 10.1016/j.supflu.2007.08.006.

[99] J. S. Cheng, M. Tang, and Y. P. Chen, “Correlation of solid solubility for biological compounds in supercritical carbon dioxide: Comparative study using solution model and other approaches,” *Fluid Phase Equilib.*, vol. 194–197, pp. 483–491, 2002, doi: 10.1016/S0378-3812(01)00657-4.

[100] M. Türk, M. Crone, and T. Kraska, “A comparison between models based on equations of state and density-based models for describing the solubility of solutes in CO2,” *J. Supercrit. Fluids*, vol. 55, no. 2, pp. 462–471, 2010, doi: 10.1016/j.supflu.2010.08.011.

[101] A. A. el Hadj, C. Si-Moussa, S. Hanini, and M. Laidi, “Application of PC-SAFT and cubic equations of state for the correlation of solubility of some pharmaceutical and statin drugs in SC-CO2,” *Chem. Ind. Chem. Eng. Q.* , vol. 19, no. 3, pp. 449–460, 2013, doi: 10.2298/CICEQ120407005E.

[102] M. Charoenchaitrakool, F. Dehghani, N. R. Foster, and H. K. Chan, “Micronization by Rapid Expansion of Supercritical Solutions to Enhance the Dissolution Rates of Poorly Water-Soluble Pharmaceuticals,” *Ind. Eng. Chem. Res*, vol. 39, p. 4794-4802, 2000, doi: 10.1021/ie000151a.

[103] S. Zabihi *et al.*, “Measuring salsalate solubility in supercritical carbon dioxide: Experimental and thermodynamic modelling,” *J. Chem. Thermodyn.*, vol. 152, p. 106271, 2021, doi: 10.1016/j.jct.2020.106271.

[104] M. Lindenberg, S. Kopp, and J. B. Dressman, “Classification of orally administered drugs on the World Health Organization Model list of Essential Medicines according to the biopharmaceutics classification system,” *Eur. J. Pharm. Biopharm.*, vol. 58, no. 2, pp. 265–278, 2004, doi: 10.1016/j.ejpb.2004.03.001.

[105] M. A. Filippa and E. I. Gasull, “Ibuprofen solubility in pure organic solvents and aqueous mixtures of cosolvents: Interactions and thermodynamic parameters relating to the solvation process,” *Fluid Phase Equilib.*, vol. 354, pp. 185–190, 2013, doi: 10.1016/j.fluid.2013.06.032.

[106] F. Espitalier, B. Biscans, and C. Laguérie, “Physicochemical Data on Ketoprofen in Solutions,” *J. Chem. Eng. Data*, vol. 40, no. 6, pp. 1222–1224, 1995, doi: 10.1021/je00022a016.

[107] A. E. Ribeiro, N. S. Graça, L. S. Pais, and A. E. Rodrigues, “Preparative separation of ketoprofen enantiomers: Choice of mobile phase composition and measurement of competitive adsorption isotherms,” *Sep. Purif. Technol.*, vol. 61, no. 3, pp. 375–383, 2008, doi: 10.1016/j.seppur.2007.11.010.

[108]; Loida Nguyen Kenneth Anderson; Lance Wherle; Min Park, ; Kenneth Nelson, “Salsalate, an Old, Inexpensive Drug with Potential New Indications: A Review of the Evidence from 3 Recent Studies,” *Am Health drug benefits*, vol. 7, no. 4, pp. 231–235, 2014.

[109] S. Wang, Z. Song, J. Wang, Y. Dong, and M. Wu, “Solubilities of Ibuprofen in Different Pure Solvents,” *J. Chem. Eng. Data*, vol. 55, pp. 5283–5285, 2010, doi: 10.1021/je100255z.

[110] S. Gracin, A. ° Ke, and C. Rasmuson, “Solubility of Phenylacetic Acid, p-Hydroxyphenylacetic Acid, p-Aminophenylacetic Acid, p-Hydroxybenzoic Acid, and Ibuprofen in Pure Solvents,” *J. Chem. Eng. Data*, vol. 47, pp. 1379–1383, 2002, doi: 10.1021/je0255170.

[111] R. Soto, M. Svärd, V. Verma, L. Padrela, K. Ryan, and Å. C. Rasmuson, “Solubility and thermodynamic analysis of ketoprofen in organic solvents,” *Int. J. Pharm.*, vol. 588, p. 119686, 2020, doi: 10.1016/j.ijpharm.2020.119686.

[112] I. Ushiki, R. Fujimitsu, and S. Takishima, “Predicting the solubilities of metal acetylacetonates in supercritical CO2: Thermodynamic approach using PC-SAFT,” *J. Supercrit. Fluids*, vol. 164, p. 104909, 2020, doi: 10.1016/j.supflu.2020.104909.

[113] “NIST Chemistry WebBook.” https://webbook.nist.gov/chemistry/ (accessed Jan. 08, 2023).

[114] M. S. Wertheim, “Fluids with highly directional attractive forces. IV. Equilibrium polymerization,” *J. Stat. Phys.*, vol. 42, no. 3–4, pp. 477–492, 1986, doi: 10.1007/BF01127722.

[115] M. S. Wertheim, “Fluids with Highly Directional Attractive Forces . III.Multiple Attraction forces,” *J. Stat. Phys.* vol. 42, no. 3–4, pp. 477–492, 1986.

[116] M. S. Wertheim, “Fluids with highly directional attractive forces. I.Statistical Thermodynamics,” *J. Stat. Phys.*, vol. 42, no. 3–4, pp. 477–492, 1986, doi:

10.1007/BF01127722.

[117] M. S. Wertheim, “Fluids with highly directional attractive forces. II. Thermodynamic Perturbation Theory and Integral Equations,” *J. Stat. Phys.*, vol. 35, no. 1–2, pp. 19–34, 1984, doi: 10.1007/BF01017362.

[118] M. Kleiner, F. Tumakaka, and G. Sadowski, “Thermodynamic modeling of complex systems,” *Struct. Bond.*, vol. 131, pp. 75–108, 2009, doi: 10.1007/978-3-540-69116-7_2.

[119] A. Ayad, A. Negadi, and F. Mutelet, “Carbon dioxide solubilities in tricyanomethanide-based ionic liquids: Measurements and PC-SAFT modeling,” *Fluid Phase Equilib.*, vol. 469, pp. 48–55, 2018, doi: 10.1016/j.fluid.2018.04.020.

[120] M. Assareh, C. Ghotbi, M. Tavakkoli, and G. Bashiri, “PC-SAFT modeling of petroleum reservoir fluid phase behavior using new correlations for petroleum cuts and plus fractions,” *Fluid Phase Equilib.*, vol. 408, pp. 273–283, 2016, doi: 10.1016/j.fluid.2015.10.032.

[121] R. Aitbelale, Y. Chhiti, F. E. M. hamdi Alaoui, A. Sahib Eddine, N. Munõz Rujas, and F. Aguilar, “High-Pressure Soybean Oil Biodiesel Density: Experimental Measurements, Correlation by Tait Equation, and Perturbed Chain SAFT (PC-SAFT) Modeling,” *J. Chem. Eng. Data*, vol. 64, no. 9, pp. 3994–4004, 2019, doi: 10.1021/acs.jced.9b00391.

[122] F. Tumakaka and G. Sadowski, “Application of the Perturbed-Chain SAFT equation of state to polar systems,” *Fluid Phase Equilib.*, vol. 217, no. 2, pp. 233–239, 2004, doi: 10.1016/j.fluid.2002.12.002.

[123] R. Favareto *et al.*, “Experimental data and thermodynamics modeling (PC-SAFT EoS) of the {CO2 + chloroform + PHBV} system at high pressures,” *J. Supercrit. Fluids*, vol. 170, p. 105140, 2021, doi: 10.1016/j.supflu.2020.105140.

[124] T. Spyriouni, X. Krokidis, and I. G. Economou, “Thermodynamics of pharmaceuticals: Prediction of solubility in pure and mixed solvents with PC-SAFT,” *Fluid Phase Equilib.*, vol. 302, no. 1–2, pp. 331–337, 2011, doi: 10.1016/j.fluid.2010.08.029.

[125] C. M. Wassvik, A. G. Holmén, C. A. S. Bergström, I. Zamora, and P. Artursson, “Contribution of solid-state properties to the aqueous solubility of drugs,” *Eur. J. Pharm. Sci.*, vol. 29, no. 3-4 SPEC. ISS., pp. 294–305, 2006, doi: 10.1016/j.ejps.2006.05.013.

[126] J. J. M. Ramos, H. P. Diogo, M. H. Godinho, C. Cruz, and K. Merkel, “Anomalous thermal behavior of salicylsalicylic acid and evidence for a monotropic transition to a nematic phase,” *Journal of Physical Chemistry B*, vol. 108, no. 23, pp. 7955–7962, 2004, doi: 10.1021/jp049903v.

[127] M. Habgood, R. W. Lancaster, M. Gateshki, and A. M. Kenwright, “The amorphous form of salicylsalicylic acid: Experimental characterization and computational predictability,” *Cryst. Growth. Des.*, vol. 13, no. 4, pp. 1771–1779, 2013, doi: 10.1021/cg400109j.

[128] B. E. Poling and J. M. Prausnitz, *The properties of gases and liquids*, 5th ed., no. C. McGraw-Hill, New York, US, 2000.

[129] G. L. Perlovich, S. v. Kurkov, A. N. Kinchin, and A. Bauer-Brandl, “Thermodynamics

of Solutions IV: Solvation of Ketoprofen in Comparison with other NSAIDs," *J. Pharm. Sci.*, vol. 92, no. 12, pp. 2502–2511, 2003, doi: 10.1002/jps.10512.

[130] D. H. Lyman, Warren J and Reehl, William F and Rosenblatt, "Handbook of chemical property estimation methods".

[131] M. T. Vieyra-Eusebio and A. Rojas, "Vapor pressures and sublimation enthalpies of nickelocene and cobaltocene measured by thermogravimetry," *J. Chem. Eng. Data*, vol. 56, no. 12, pp. 5008–5018, 2011, doi: 10.1021/je200815v.

[132] H. Bagheri, S. Ghader, and N. Hatami, "Solubility of ibuprofen in conventional solvents and supercritical co 2 : evaluation of ideal and non-ideal models," *Chem. Chem. Technol.*, vol. 13, no. 1, pp. 1–10, 2019, doi: 10.23939/chcht13.01.001.

[133] A. Rashid, E. T. White, T. Howes, J. D. Litster, and I. Marziano, "Effect of Solvent Composition and Temperature on the Solubility of Ibuprofen in Aqueous Ethanol," *J. Chem. Eng. Data*, vol. 59, pp. 2699-2703, 2014, doi: 10.1021/je400819z.

[134] D. P. Pacheco, Y. J. Manrique, and F. Martínez, "Thermodynamic study of the solubility of ibuprofen and naproxen in some ethanol + propylene glycol mixtures," *Fluid Phase Equilib.*, vol. 262, no. 1–2, pp. 23–31, 2007, doi: 10.1016/j.fluid.2007.07.076.

[135] J. Brinkmann, F. Huxoll, C. Luebbert, and G. Sadowski, "Solubility of pharmaceutical ingredients in triglycerides," *Eur. J. Pharm. Biopharm.*, vol. 145, pp. 113–120, 2019, doi: 10.1016/j.ejpb.2019.10.012.

[136] J. Nerurkar, J. W. Beach, M. O. Park, and H. W. Jun, "Solubility of (±)-Ibuprofen and S ( )-Ibuprofen in the Presence of Cosolvents and Cyclodextrins," *Pharm. Dev.*

Technol., vol. 10, no. 3, pp. 413–421, 2005, doi: 10.1081/pdt-200054446.

[137] K. B. Smith, R. H. Bridson, G. A. Leeke, and † Glaxosmithkline, "Solubilities of Pharmaceutical Compounds in Ionic Liquids," *J. Chem. Eng. Data*, vol. 56, pp. 2039–2043, 2011, doi: 10.1021/je101040p.

[138] A. Jouyban, S. Soltanpour, and W. E. Acree, "Solubility of Acetaminophen and Ibuprofen in the Mixtures of Polyethylene Glycol 200 or 400 with Ethanol and Water and the Density of Solute-Free Mixed Solvents at 298.2 K," *J. Chem. Eng. Data*, vol. 55, pp. 5252–5257, 2010, doi: 10.1021/je100829d.

[139] W. Dun, S. Wu, X. Wang, D. Sun, S. Du, and J. Gong, "Solubility of Ibuprofen Sodium Dihydrate in Acetone + Water Mixtures: Experimental Measurement and Thermodynamic Modeling," *J. Chem. Eng. Data*, vol. 59, pp. 3415–3421, 2014, doi: 10.1021/je5004093.

[140] J. Manrique and F. Martínez, "Solubility of ibuprofen in some ethanol + water cosolvent mixtures at several temperatures," *Lat. Am. J. Pharm.*, vol. 26, no. 3, pp. 344–354, 2007.

[141] L. C. Garzón and F. Martínez, "Temperature dependence of solubility for ibuprofen in some organic and aqueous solvents," *J. Solution Chem.*, vol. 33, no. 11, pp. 1379–1395, 2004, doi: 10.1007/s10953-004-1051-2.

[142] P. Bustamante, M. A. Peña, and J. Barra, "The modified extended Hansen method to determine partial solubility parameters of drugs containing a single hydrogen bonding group and their sodium derivatives: Benzoic acid/Na and ibuprofen/Na," *Int. J. Pharm.*, vol. 194, no. 1, pp. 117–124, 2000, doi: 10.1016/S0378-5173(99)00374-9.

[143] D. M. Aragón, J. E. Rosas, and F. Martínez, “Thermodynamic study of the solubility of ibuprofen in acetone and dichloromethane,” *Braz. J. Pharm. Sci.*, vol. 46, no. 2, pp. 227–235, 2010, doi: 10.1590/S1984-82502010000200009.

[144] G. I. Burgos-Solórzano, J. F. Brennecke, and M. A. Stadtherr, “Solubility measurements and modeling of molecules of biological and pharmaceutical interest with supercritical CO2,” *Fluid Phase Equilib.*, vol. 220, no. 1, pp. 55–67, 2004, doi: 10.1016/j.fluid.2004.01.036.

[145] M. Lashkarbolooki, A. Z. Hezave, Y. Rahnama, R. Ozlati, H. Rajaei, and F. Esmaeilzadeh, “Solubility of cyproheptadine in supercritical carbon dioxide; Experimental and modeling approaches,” *J. Supercrit. Fluids*, vol. 84, pp. 13–19, 2013, doi: 10.1016/j.supflu.2013.09.004.

Appendix I

Table S- 1. The experimental and obtained solubility of Ibuprofen in organic solvents

Solvent	T [K]	x [-] [a]	$x_{estimation}$ (k_{ij}=0)[-] [b]	$RD_{estimation}$ [%][c]	$x_{correlation}$ (k_{ij}≠0)[-] [b]	$RD_{estimation}$ [%][c]
Acetone [109]	283.57	0.1437	0.1386	3.53	0.1444	0.4917
	288.49	0.1684	0.1721	2.22	0.1684	0.0041
	293.37	0.1996	0.2097	5.06	0.1970	1.2808
	297.87	0.233	0.2481	6.48	0.2285	1.9510
	303.25	0.2732	0.2988	9.375	0.2731	0.0288
	308.07	0.3114	0.3489	12.03	0.3203	2.8681
	312.65	0.3516	0.4008	14.00	0.3719	5.7679
Ethyl Acetate [109]	283.17	0.1267	0.1474	16.34	0.1278	0.9028
	288.47	0.1584	0.1805	13.95	0.1584	0.0057
	293.57	0.1935	0.2170	12.13	0.1931	0.1854
	297.69	0.2254	0.2499	10.89	0.2254	0.0041
	302.75	0.2713	0.2950	8.72	0.2705	0.3045
	307.83	0.3195	0.3455	8.152	0.3222	0.8399
	313.07	0.3762	0.4038	7.34	0.3827	1.7303
	318.45	0.4388	0.4708	7.30	0.4529	3.2222
Toluene [110]	283.15	0.1034	0.1023	1.05	0.1059	2.3949
	288.15	0.1329	0.1299	2.28	0.1329	0.0100
	293.15	0.1696	0.1634	3.64	0.1656	2.3412
	303.15	0.2509	0.2506	0.09	0.2509	0.0018
	308.15	0.2995	0.3049	1.83	0.3043	1.6221
Chloroform [110]	283.15	0.2093	0.1166	44.30	0.2093	0.0021
	288.15	0.2429	0.1495	38.46	0.2390	1.6192
	293.15	0.2718	0.1880	30.83	0.2718	0.0005

a: Experimental solubility of ibuprofen in organic solvent.
b: Estimated solubility values for Ibuprofen in organic solvent obtained by PC-SAFT when *kij* =0
c: Correlated solubility values obtained by PC-SAFT when *kij* is used as an additional fitting parameter
d: The relative deviation between experimental and estimated values
e: The relative deviation between experimental and correlated values

Table S- 2. The experimental and obtained solubility of ketoprofen in organic solvents

Solvent	T [K]	x [-] [a]	$x_{estimation}$ (k_{ij}=0)[-] [b]	$RD_{estimation}$ [%][c]	$x_{correlation}$ (k_{ij}≠0)[-] [b]	$RD_{estimation}$ [%][c]
Acetone	279.55	0.0728	0.0363	50.1593	0.0736	1.1750
	284.30	0.0811	0.0482	40.6287	0.0811	0.0006
	288.35	0.0885	0.0602	31.9647	0.0884	0.1957
	293.2	0.0983	0.0772	21.5160	0.0983	0.0011
	297.65	0.1093	0.0952	12.9335	0.1090	0.3150
	302.85	0.1193	0.1193	0.0000	0.1236	3.6184
Ethyl Acetate [99]	278.15	0.050	0.0507	1.3083	0.0471	5.8079
	283.15	0.0550	0.0643	16.8620	0.0564	2.6303
	288.15	0.0660	0.0801	21.3263	0.0673	2.0158
	293.15	0.08	0.0982	22.7025	0.0800	0.0008
	298.15	0.0955	0.1187	24.2528	0.0948	0.7725
	303.15	0.1120	0.1417	26.5545	0.1120	0.0001
Toluene	279.65	0.0084	0.0073	13.7936	0.0077	8.8692
	284.2833	0.0105	0.0102	3.2355	0.0105	0.0011
	288.82	0.0138	0.0140	1.3636	0.0142	2.5631
	293.55	0.0194	0.0194	0.0001	0.0192	0.9107
	297.65	0.0241	0.0256	6.2386	0.0249	3.4935
	302.62	0.0341	0.0356	4.6176	0.0341	0.0013
o-Xylene	279.45	0.0058	0.0049	14.9997	0.0057	0.0006
	284.1	0.0078	0.0068	11.8810	0.0079	1.4100
	288.8	0.0110	0.0095	12.8592	0.0107	1.8386
	293.4	0.0147	0.0131	10.5987	0.0145	1.3013

a: Experimental solubility of Ketoprofen in organic solvent.
b: Estimated solubility values for Ketoprofen in organic solvent obtained by PC-SAFT when *kij* =0
c: Correlated solubility values obtained by PC-SAFT when *kij* is used as an additional fitting parameter
d: The relative deviation between experimental and estimated values
e: The relative deviation between experimental and correlated values

Table S- 3. The experimental and obtained solubility of salsalate in organic solvents

Solvent	T [K]	x [-] [a]	$x_{estimation}$ (k_{ij}=0)[-] [b]	$RD_{estimation}$ [%][c]	$x_{correlation}$ (k_{ij}≠0)[-] [b]	$RD_{estimation}$ [%][c]
Acetone	280.15	0.0736	0.0197	73.2929	0.0736	0.0004
	284.45	0.0765	0.0254	66.7531	0.0770	0.6558
	289.05	0.0808	0.0327	59.4933	0.0808	0.0013
	293.5	0.0865	0.0410	52.6581	0.0849	1.8850
	298.1	0.0906	0.0506	44.1279	0.0895	1.2096
	305.9	0.0960	0.0694	27.6847	0.0983	2.3518
Ethyl Acetate	0.0527	0.038	28.219	0.053	0.00857	0.0527
	0.0561	0.046	18.017	0.056	0.00055	0.0561
	0.0596	0.054	9.171	0.059	0.31767	0.0596
	0.0637	0.064	0.000	0.063	0.66600	0.0637
	0.0671	0.073	8.976	0.067	0.00003	0.0671
	0.0724	0.088	20.988	0.073	0.96730	0.0724
Toluene	280.05	0.0014	0.0019	29.55	0.0014	0.0016
	284.25	0.0018	0.0025	40.98	0.0018	0.0004
	288.95	0.0022	0.0034	50.71	0.0022	2.3914
	293.8	0.0026	0.0046	79.83	0.0027	6.4290
	297.7	0.0032	0.0059	87.37	0.0033	3.4048
	304.8	0.0046	0.0091	98.76	0.0044	2.8769
o-Xylene	279.7	0.0017	0.0011	39.08	0.0016	6.39
	284.1	0.0020	0.0014	26.53	0.0020	1.63
	288.8	0.0025	0.0020	19.58	0.0025	0.00
	293.4	0.0030	0.0027	11.11	0.0030	0.00
	297.9	0.0036	0.0035	1.36	0.0036	1.09
	302.9	0.0045	0.0048	6.64	0.0044	1.24

a: Experimental solubility of salsalate in organic solvent.
b: Estimated solubility values for salsalate in organic solvent obtained by PC-SAFT when *kij* =0
c: Correlated solubility values obtained by PC-SAFT when *kij* is used as an additional fitting parameter
d: The relative deviation between experimental and estimated values
e: The relative deviation between experimental and correlated values

Table S- 4. Experimental and Obtained solubilities of ibuprofen in $scCO_2$

T [K]	*P* [MPa]	ρ_{scf} [kg/m^3] [a]	*y* [-] [b]	$y_{estimation}$ (k_{ij}=0)[-] [c]	$RD_{estimation}$ [%] [e]	$y_{correlation}$ (k_{ij}≠0)[-] [d]	$RD_{estimation}$ [%] [f]
308 [102]	8.5	612.1	5.43×10^{-4}	1.16×10^{-3}	113.58	9.32×10^{-4}	71.61
	9	662.1	9.95×10^{-4}	1.78×10^{-3}	79.24	1.42×10^{-3}	42.99
	10	712.8	1.35×10^{-3}	2.30×10^{-3}	70.46	1.83×10^{-3}	35.48
	11	743.9	1.81×10^{-3}	2.75×10^{-3}	51.86	2.18×10^{-3}	20.47
	12	767.1	2.13×10^{-3}	3.14×10^{-3}	47.48	2.49×10^{-3}	16.90
	13	785.7	2.5×10^{-3}	3.49×10^{-3}	39.56	2.76×10^{-3}	10.58
	14	801.4	2.43×10^{-3}	3.8×10^{-3}	56.32	3.01×10^{-3}	23.87
	15	815.1	2.68×10^{-3}	4.08×10^{-3}	52.07	3.23×10^{-3}	20.52
	16	827.2	3.23×10^{-3}	4.32×10^{-3}	33.85	3.43×10^{-3}	6.12
	17	838.1	3.82×10^{-3}	4.55×10^{-3}	19.01	3.61×10^{-3}	5.61
	18	848.1	3.78×10^{-3}	4.93×10^{-3}	30.35	3.91×10^{-3}	3.46
	20	865.7	4.23×10^{-3}	5.23×10^{-3}	23.80	4.15×10^{-3}	1.67
	22	881.1	4.41×10^{-3}	5.24×10^{-3}	18.74	4.16×10^{-3}	5.68
313 [102]	9.5	580.1	5.85×10^{-4}	5.49×10^{-4}	6.10	5.93×10^{-4}	1.431
	12	717.7	2.32×10^{-3}	2.18×10^{-3}	5.93	2.39×10^{-3}	2.971
	14	763.3	3.18×10^{-3}	3.15×10^{-3}	0.83	3.46×10^{-3}	8.702
	17	807.9	4.67×10^{-3}	4.26×10^{-3}	8.81	4.66×10^{-3}	0.119
	20	839.8	6.80×10^{-3}	5.06×10^{-3}	25.55	5.54×10^{-3}	18.56
	22	857.2	6.49×10^{-3}	5.48×10^{-3}	15.61	5.99×10^{-3}	7.772
318 [102]	8.5	281.8	3.00×10^{-5}	1.50×10^{-5}	49.78	1.72×10^{-5}	42.73
	9	337.5	4.00×10^{-5}	3.11×10^{-5}	22.16	3.62×10^{-5}	9.411
	9.5	414.6	1.13×10^{-4}	7.89×10^{-5}	30.14	9.47×10^{-5}	16.17
	10	498.3	3.02×10^{-4}	2.30×10^{-4}	23.85	2.90×10^{-4}	3.929
	11	603.2	1.29×10^{-3}	8.34×10^{-4}	35.34	1.14×10^{-3}	11.95
	12	657.7	2.00×10^{-3}	1.49×10^{-3}	25.59	2.09×10^{-3}	4.557
	14	720.5	3.74×10^{-3}	2.67×10^{-3}	28.60	3.83×10^{-3}	2.390
	17	775.5	5.84×10^{-3}	4.08×10^{-3}	30.18	5.84×10^{-3}	0.001

a: Density of $scCO_2$

b: The experimental solubility of ibuprofen in $scCO_2$ [102]

c: The estimated solubility for ibuprofen in $scCO_2$ obtained by PC-SAFT when k_{ij} =0

d: The correlated solubility of ibuprofen in $scCO_2$ by PC-SAFT when k_{ij} is used as an additional fitting parameter

e: The relative deviation when k_{ij} in Eq. (3-5) is set to zero.

f: The relative deviation when k_{ij} in Eq. (3-5) is used as an additional fitting parameter.

Table S- 5 Experimental and Obtained solubilities of ketoprofen in $scCO_2$

T [K]	*P* [MPa]	ρ_{scf} [kg/m^3] [a]	*y* [-] [b]	$y_{estimation}$ (k_{ij}=0)[-] [c]	$RD_{estimation}$ [%] [e]	$y_{correlation}$ (k_{ij}≠0)[-] [d]	$RD_{estimation}$ [%] [f]
308	16	827.2	2.21×10^{-5}	2.21×10^{-5}	0.00	1.85×10^{-5}	16.40
[57]	20	865.7	2.56×10^{-5}	3.01×10^{-5}	17.60	2.49×10^{-5}	2.578
	24	894.9	2.87×10^{-5}	3.70×10^{-5}	28.92	3.05×10^{-5}	6.051
	28	918.6	3.21×10^{-5}	4.29×10^{-5}	33.68	3.51×10^{-5}	9.323
	32	938.8	3.45×10^{-5}	4.79×10^{-5}	38.97	3.90×10^{-5}	13.09
	36	956.5	4.23×10^{-5}	5.22×10^{-5}	23.43	4.23×10^{-5}	0.001
	40	972.3	4.56×10^{-5}	5.58×10^{-5}	22.36	4.50×10^{-5}	1.256
318	16	759.9	5.01×10^{-5}	2.21×10^{-5}	55.98	3.17×10^{-5}	36.75
[57]	20	812.7	6.58×10^{-5}	3.56×10^{-5}	45.87	5.26×10^{-5}	20.08
	24	849.4	7.68×10^{-5}	4.79×10^{-5}	37.58	7.22×10^{-5}	6.020
	28	878	9.01×10^{-5}	5.89×10^{-5}	34.59	9.01×10^{-5}	0.002
	32	901.7	1.12×10^{-4}	6.86×10^{-5}	38.72	1.06×10^{-4}	5.116
	36	922	1.03×10^{-4}	7.71×10^{-5}	25.13	1.21×10^{-4}	17.19
	40	939.8	1.20×10^{-4}	8.45×10^{-5}	29.61	1.34×10^{-4}	11.25
328	16	681.1	7.01×10^{-5}	1.89×10^{-5}	73.10	4.31×10^{-5}	38.49
[57]	20	754.6	1.16×10^{-4}	3.85×10^{-5}	66.82	9.67×10^{-5}	16.63
	24	801.1	1.75×10^{-4}	5.80×10^{-5}	66.85	1.55×10^{-4}	11.44
	28	835.7	2.20×10^{-4}	7.64×10^{-5}	65.29	2.14×10^{-4}	2.922
	32	863.3	2.54×10^{-4}	9.32×10^{-4}	63.32	2.70×10^{-4}	6.420
	36	886.6	3.24×10^{-4}	1.08×10^{-4}	66.57	3.24×10^{-4}	0.006
	40	906.7	3.59×10^{-4}	1.22×10^{-4}	66.06	3.74×10^{-4}	4.213
331	11.56	424.3	7.80×10^{-6}	1.62×10^{-6}	79.29	3.29×10^{-6}	57.85
[55]	13	531.3	1.63×10^{-5}	4.92×10^{-6}	69.80	1.16×10^{-5}	29.04
	16	655.2	5.50×10^{-5}	1.76×10^{-5}	67.96	4.98×10^{-5}	9.417
	19	720.1	1.05×10^{-4}	3.34×10^{-5}	68.19	1.05×10^{-4}	0.001
	22	763.5	1.55×10^{-4}	4.99×10^{-5}	67.82	1.69×10^{-4}	8.874
338	16	592.4	1.01×10^{-4}	1.50×10^{-5}	85.12	4.60×10^{-5}	54.49
[57]	20	691.7	2.45×10^{-4}	3.92×10^{-5}	83.99	1.44×10^{-4}	41.13
	24	750.4	3.25×10^{-4}	6.68×10^{-5}	79.43	2.76×10^{-4}	15.12
	28	791.9	4.92×10^{-4}	9.47×10^{-5}	80.76	4.24×10^{-4}	13.77
	32	824.2	5.79×10^{-4}	1.21×10^{-4}	79.04	5.79×10^{-4}	0.002
	36	850.8	6.87×10^{-4}	1.46×10^{-4}	78.72	7.33×10^{-4}	6.758
	40	873.4	7.12×10^{-4}	1.69×10^{-4}	76.26	8.83×10^{-4}	24.06

a: Density of $scCO_2$, b: The experimental solubility of ketoprofen in $scCO_2$ [102]
c: The estimated solubility for ketoprofen in $scCO_2$ obtained by PC-SAFT when k_{ij} =0
d: The correlated solubility of ketoprofen in $scCO_2$ by PC-SAFT when k_{ij} is used as an additional fitting parameter, e: The relative deviation when k_{ij} in Eq. (3-5) is set to zero.
f: The relative deviation when k_{ij} in Eq. (3-5) is used as an additional fitting parameter

Table S- 6 Experimental and Obtained solubilities of salsalate in $scCO_2$

T [K]	P [MPa]	ρ_{scf} [kg/m^3] [a]	y [-] [b]	$y_{estimation}$ (k_{ij}=0)[-] [c]	$RD_{estimation}$ [%] [e]	$y_{correlation}$ ($k_{ij}\neq0$)[-] [d]	$RD_{estimation}$ [%] [e]
308	12	768.4	1.07×10^{-4}	1.26×10^{-4}	18.03	1.17×10^{-4}	9.378
[103]	16	828.1	1.98×10^{-4}	2.14×10^{-4}	8.51	1.98×10^{-4}	0.001
	20	866.5	2.47×10^{-4}	2.81×10^{-4}	13.81	2.58×10^{-4}	4.519
	24	895.5	2.95×10^{-4}	3.28×10^{-4}	11.19	3.00×10^{-4}	1.851
	28	919.2	3.88×10^{-4}	3.59×10^{-4}	7.49	3.28×10^{-4}	15.43
	32	939.4	4.71×10^{-4}	3.77×10^{-4}	19.95	3.44×10^{-4}	26.95
	36	957	5.35×10^{-4}	3.85×10^{-4}	28.01	3.51×10^{-4}	34.42
	40	972.7	5.77×10^{-4}	3.85×10^{-4}	33.19	3.51×10^{-4}	39.24
318	12	659.7	7.07×10^{-5}	9.41×10^{-5}	33.06	8.17×10^{-5}	15.58
[103]	16	828.1	2.17×10^{-4}	2.82×10^{-4}	30.09	2.40×10^{-4}	10.64
	20	813.5	3.59×10^{-4}	4.47×10^{-4}	24.57	3.77×10^{-4}	4.89
	24	850.1	4.83×10^{-4}	5.77×10^{-4}	19.49	4.83×10^{-4}	0.001
	28	878.6	6.74×10^{-4}	6.73×10^{-4}	0.13	5.61×10^{-4}	16.79
	32	902.2	8.59×10^{-4}	7.43×10^{-4}	13.89	6.14×10^{-4}	28.52
	36	922.5	9.58×10^{-4}	7.82×10^{-4}	18.38	6.47×10^{-4}	32.47
	40	940.2	1.28×10^{-3}	8.05×10^{-4}	37.15	6.64×10^{-4}	48.15
328	12	506.9	6.12×10^{-5}	4.07×10^{-5}	33.45	3.83×10^{-5}	37.42
[103]	16	828.1	1.87×10^{-4}	3.05×10^{-4}	63.06	2.81×10^{-4}	50.22
	20	755.5	5.14×10^{-4}	6.31×10^{-4}	22.82	5.77×10^{-4}	12.23
	24	801.9	6.85×10^{-4}	9.23×10^{-4}	34.71	8.40×10^{-4}	22.61
	28	836.3	1.05×10^{-3}	1.16×10^{-3}	10.10	1.05×10^{-3}	0.01
	32	864	1.39×10^{-3}	1.31×10^{-3}	4.26	1.21×10^{-3}	13.18
	36	887.1	1.69×10^{-3}	1.46×10^{-3}	13.96	1.32×10^{-3}	22.06
	40	907.2	2.25×10^{-3}	1.53×10^{-3}	31.79	1.39×10^{-3}	38.28
338	12	384.2	3.77×10^{-5}	2.98×10^{-5}	20.89	2.74×10^{-5}	27.13
[103]	16	593.74	1.66×10^{-4}	2.96×10^{-4}	78.85	2.63×10^{-4}	58.68
	20	692.7	5.93×10^{-4}	8.20×10^{-4}	38.33	7.14×10^{-4}	20.39
	24	751.2	1.02×10^{-3}	1.38×10^{-3}	35.06	1.19×10^{-3}	16.55
	28	792.6	1.60×10^{-3}	1.86×10^{-3}	16.28	1.60×10^{-3}	0.011
	32	824.8	2.11×10^{-3}	2.24×10^{-3}	6.16	1.92×10^{-3}	8.833
	36	851.3	2.52×10^{-3}	2.52×10^{-3}	0.01	2.16×10^{-3}	14.16
	40	874	3.88×10^{-4}	2.72×10^{-3}	30.02	2.33×10^{-3}	39.95

a: Density of $scCO_2$ calculated

b: The experimental solubility of salsalate in $scCO_2$

c: The estimated solubility for salsalate in $scCO_2$ obtained by PC-SAFT when k_{ij} =0

d: The correlated solubility of salsalate in $scCO_2$ by PC-SAFT when k_{ij} is used as an additional fitting parameter

e: The relative deviation when k_{ij} in Eq. (3-5) is set to zero.

e: The relative deviation when k_{ij} in Eq. (3-5) is used as an additional fitting parameter.

Appendix II: List of Tables